

Two-photon decay rates of hydrogenlike ions revisited by using Dirac-Coulomb Sturmian expansions of the first order

Zachée Bona,¹ Hugues Merlain Tetchou Nganso,¹ Thierry Blanchard Ekogo,² and Moïse Godfroy Kwato Njock^{1,*}

¹Centre for Atomic Molecular Physics and Quantum Optics (CEPAMOQ), Faculty of Science, University of Douala, P.O. Box 8580, Douala, Cameroon

²Département de Physique, Faculté des Sciences, Université des Sciences et Techniques de Masuku, B.P. 943 Franceville, Gabon

(Received 29 September 2013; published 19 February 2014)

A fully relativistic multipole scheme is formulated to study two-photon emission processes in hydrogenlike ions with an infinitely heavy, pointlike, and spinless nucleus of charge up to 100. By making use of the Sturmian expansion of the Dirac-Coulomb Green function of the first order constructed by Szmtykowski, closed-form expressions are derived for arbitrary multipole channels. In the nonrelativistic limit, well-known formulas established previously are retrieved. For the sake of assessing the effectiveness of our approach, numerical applications are then carried out for two-photon decay rates of the selected $2s_{1/2}$ and $2p_{1/2}$ atomic states. To this end, radial integrals, the most crucial quantities involved in the matrix elements, are treated with great care by means of two suitable techniques that agree with each other quite closely so that very accurate values are obtained regardless of the choice of parameters, such as radial quantum numbers and orders of spherical Bessel functions of the first kind. In addition, the convergence and stability of computations are checked in connection with the intermediate-state summation, which appears within the second-order perturbation theory. As expected, the gauge invariance of our fully relativistic multipole numbers is confirmed. Relativistic effects, and the influence of the negative spectrum of the complete set of Dirac-Coulomb Sturmians of first order and retardation truncations in the transition operator are examined. Finally, a comparison is undertaken of our two-photon relativistic calculations with refined predictions of other authors based on finite basis-set methods widely employed over the past decades.

DOI: 10.1103/PhysRevA.89.022514

PACS number(s): 31.30.J-, 32.70.Fw, 32.80.Wr

I. INTRODUCTION

Two-photon transitions in atomic systems, e.g., two-photon decay and absorption [1–3], Raman and Rayleigh scattering [4,5], and so on, have been under investigation both experimentally [6–9] and theoretically since the advent of quantum mechanics. To be specific, they have become a useful and even a standard tool for experimental studies of various spectroscopic characteristics in atoms [10,11], excitation levels of various systems [12], composition and structure of materials, as well as many other applications such as the determination of physical constants [13–15], measurement of the Lamb shift [8,14], parity-violation phenomena [16,17], and test of Bell's inequality and hidden-variable theories [18,19]. Two-photon transitions are also of interest in astrophysics [20,21], molecular spectroscopy [22], tissue imaging [23], and protein structure analysis [24]. In connection with experimental studies, these processes have been the subject of a large number of theoretical papers. Since the seminal works of Kramers and Heisenberg [25], Waller [26], and Goeppert-Mayer [27], there has been continuing interest in accurate calculations of two-photon decay in hydrogenlike ions. The first application of the mathematical formalism found in Goppert-Mayer's doctoral thesis [27] to the case of the $2s \rightarrow 1s$ transition in atomic hydrogen was performed by Breit and Teller [28]. Their rough evaluation confirmed that among the two competitive processes, namely, the emission of two electric dipole photons ($2E1$) and the emission of a single-photon magnetic dipole ($M1$), the two-photon branch dominates by far in the radiative decay of the $2s$ metastable state and is therefore the principal

cause of the mechanism of decay of interstellar $2s$ hydrogen atoms. Within the framework of nonrelativistic approximation, other subsequent detailed calculations including the shape of the emitted spectrum were done, so that more accurate estimates were obtained progressively by a number of authors, for instance, Spitzer and Greenstein [29], Shapiro and Breit [30], Zon *et al.* [31], and Klarsfeld [32]. In the nonrelativistic dipole approximation, Tung *et al.* [33] and Florescu [34] calculated two-photon emission rates from higher shells $ns = 3s - 6s$ and $3s, 3d$, respectively, in hydrogenic atoms. Labzowsky *et al.* evaluated the $E1M1$ and $E1E2$ emission probabilities for the $2p \rightarrow 1s$ transition [35,36]. The problem of the choice of gauge in two-photon transitions has been discussed as well by many authors [37–39]. In heavy ions and atoms, relativistic and quantum electrodynamic (QED) effects become of paramount importance and, as a result, they may strongly affect the properties of two-photon emission. The first fully relativistic calculation of two-photon decay rates was done by Johnson [40]. Other investigations based on the Dirac equation and including all relativistic and retardation effects and all combinations of photon multipoles have been carried out for total decay rates and spectral distributions [41–47], as well as for the angular and polarization correlations [48–50].

It is well known that a two-photon process proceeds via intermediate states. In practice, the main difficulty encountered in the computation of amplitudes of second order comes from summations over the complete spectrum of the system under consideration. Several adequate approximation techniques have been developed over the past decades to evaluate these sums consistently. Among others, one can cite the implicit technique introduced by Dalgarno and Lewis [51] and generalized by Gontier and Trahin [52] to the cases where the number of photons involved in the process is greater than two.

*mkwato@yahoo.com

It involves, however, elaborate numerical methods, especially for higher-order calculations. Bebb and Gold [53] defined an average frequency thereby replacing the infinite summation by an average term and using the closure property of the wave functions to remove the intermediate-state transitions from the problem. Another approach, which has proven to be of remarkable efficiency, is the discrete-basis-set method [39,41,42,44,54–56]. If it is successful, its advantage lies in the replacement of the infinite sums by a finite sum over tractable and square-integrable pseudostates. In many applications, the so-called pseudostate summation technique has required only a very small number of terms to achieve high accuracy. An alternative accurate method advocated during the past decades is based on the Coulomb Green function (CGF). Various representations of that object of fundamental importance have been reported in the literature, starting with the pioneering nonrelativistic works of Schwinger [57] and Hostler [58]. The CGF method was first applied by Zon *et al.* [31] and Klarsfeld [32] in hydrogen and hydrogenlike ions for deriving the general expression for two-photon decay probabilities. In addition, the Schrödinger-Coulomb Green function expressed in the Sturmian representation and introduced by Hostler [59] has emerged as a very useful and powerful tool of attack for studying low-Z ions. It is known analytically and yields, in a natural and straightforward calculation, analytical expressions of the desired amplitudes [60,61], with summation of rapidly convergent series. The advantages of this representation have been recognized by a number of authors, who used it also in the computation of higher-order atomic processes [35,62]. Note that the CGF may be built up from the Schrödinger-Coulomb Sturmians [63]. These functions were originally introduced by Holøien [64] and Shull and Löwdin into quantum chemistry [65]. The term “Sturmian” has no historical significance and was a whim of Rotenberg [66] in order to emphasize their connection with Sturm-Liouville theory. These Sturmians, which are well adapted to numerical tasks, are nowadays one of the most commonly used functional basis sets. They have been successfully employed in many atomic physics studies [67–69]. Thus the fact that the Schrödinger-Coulomb Sturmians and Schrödinger-Coulomb Green functions proved to be a valuable tool led to the construction of their relativistic counterparts for applications in relativistic atomic and molecular physics. It is in this context that Drake and Goldman [70] and Quiney and Grant [71] derived bispinor bases, which played a major role in developing techniques for solving Dirac-Fock(-Breit) equations for atoms and molecules, and related problems in quantum electrodynamics.

Later, Szmytkowski [72,73] claimed that the relativistic bases of these authors should not be considered a Sturmian set, and he generalized their ideas to derive complete sets of Dirac-Coulomb Sturmians and the series expansion of the Dirac-Coulomb Green function associated directly with first-order Sturm-Liouville problems. However, it is worth mentioning that Grant and Quiney [74] pointed out that Szmytkowski’s description of their work, based on a limited published material, was misleading. In a remarkable series of papers, Szmytkowski illustrated the applicability, utility, and efficiency of these Sturmian expansions by computing the static electric dipole polarizability [72,75], the dynamic dipole polarizability tensor [76], the magnetizability [77], and the

Stark-induced magnetic anapole moment [78] of relativistic hydrogenlike ions in the ground state. Further examples of the utility of the first-order Sturmian expansion of the Dirac-Coulomb Green function have been presented by this author in two recent papers [79,80]. The motivation of this work stems from that point. Accordingly, it is the purpose of the present contribution to explore the usefulness and effectiveness, in a different sort of problem, of the Dirac-Coulomb Sturmians and Coulomb Green function reported by Szmytkowski. It follows the calculations in the previous one [81] and is devoted to a reevaluation of two-photon spontaneous-emission rates of the nonresonant $2p_{1/2}$ and $2s_{1/2}$ states for hydrogenic atoms [45], with an infinitely heavy, pointlike, and spinless nucleus of charge Z ranging from 1 to 100.

We organize the material as follows. Section II describes the essentials of the general theory of two-photon spontaneous-emission rates. We analytically provide, in closed form, relevant relativistic expressions in the length and velocity gauges, with application to some transition probabilities. These transitions have been selected in connection with Sec. III in which the nonrelativistic treatment is presented and the fact that there are misprints in the corresponding formulas in Ref. [35]. Details on matrix elements and radial integrals for emission and absorption are included in Appendices A and B. Section IV is devoted to the presentation and discussion of our numerical results. Finally, in Sec. V, we make some concluding remarks. Notice that atomic units (a.u. : $\hbar = m = e = 1, c = 1/\alpha$) and relativistic atomic units (r.a.u. : $\hbar = m = c = 1, e^2 = \alpha$) are used throughout, and α stands for the fine-structure constant. The values of these fundamental constants used for conversion in the tables are given in Ref. [82]. Note also that the units of time in atomic and relativistic atomic units are $\tau_0^{(NR)} = a_0/(\alpha c)$ and $\tau_0^{(R)} = \alpha^2 \tau_0^{(NR)} = \alpha a_0/c$, respectively, where a_0 is the Bohr radius.

II. GENERAL THEORY OF RELATIVISTIC TWO-PHOTON DECAY RATES

In this section, we obtain, in a computationally convenient form, exact analytical formulas of two-photon decay rates for hydrogenlike ions using the Sturmian expansion of the Dirac-Coulomb Green (DCG) function of the first order derived by Szmytkowski [72].

A. General formalism

Following the treatment presented in our previous work within the framework of quantum electrodynamics [81], the basic expression for the S -matrix element corresponding to the emission of two photons can be written in the form

$$S_{fi} = 2\pi i \delta(E_i - E_f - \omega_1 - \omega_2) U_{fi}, \quad U_{fi} = U_{fi}^{(1)} + U_{fi}^{(2)}, \quad (1)$$

$$U_{fi}^{(1)} = \int d^3 \mathbf{r}_1 d^3 \mathbf{r}_2 \Psi_f^\dagger(\mathbf{r}_2) V(\mathbf{r}_2, \mathbf{k}_2) G_E(\mathbf{r}_2, \mathbf{r}_1) \times V(\mathbf{r}_1, \mathbf{k}_1) \Psi_i(\mathbf{r}_1), \quad (2)$$

$$U_{fi}^{(2)} = \int d^3\mathbf{r}_1 d^3\mathbf{r}_2 \Psi_f^\dagger(\mathbf{r}_2) V(\mathbf{r}_2, \mathbf{k}_1) G_E(\mathbf{r}_2, \mathbf{r}_1) \times V(\mathbf{r}_1, \mathbf{k}_2) \Psi_i(\mathbf{r}_1), \quad (3)$$

where the indices i and f denote the initial and final unperturbed Dirac hydrogenic bound states, respectively. The dagger means the Hermitian conjugate. $G_E(\mathbf{r}_2, \mathbf{r}_1)$ represents the first-order Dirac-Coulomb Green function in the three-dimensional space, with energy parameter E of the intermediate states. The necessary formulas for bispinor wave functions and DCG functions are given in Appendix A in a form which is very useful for actual calculations. The transition operators $V(\mathbf{r}, \mathbf{k}_j)$ with $j = 1, 2$ describe the interaction of the electron with the electromagnetic field [41]. \mathbf{k}_j is the wave vector for the emitted j th photon of frequency ω_j . The δ -function factor expresses the energy-conservation law $E_i - E_f = \omega_1 + \omega_2$, from which it appears that the emission spectrum is continuous.

Considering the well-known transition probability averaged over m_i and summed over m_f ion magnetic sublevels,

$$d^6W^{(R)} = \frac{2\pi}{2j_i + 1} \left(\sum_{m_i, m_f} |U_{fi}|^2 \right) \times \delta(E_i - E_f - \omega_1 - \omega_2) \frac{d^3\mathbf{k}_1}{(2\pi)^3} \frac{d^3\mathbf{k}_2}{(2\pi)^3}, \quad (4)$$

and integrating, over the frequency ω_2 , the elements of solid angle $d^2\hat{\mathbf{k}}_1, d^2\hat{\mathbf{k}}_2$, and summing over the polarization vectors, leads to the total average decay rate in relativistic atomic units,

$$\frac{dW^{(R)}}{d\omega_1} = \frac{\alpha^2 \omega_1 \omega_2}{(2\pi)^3 (2j_i + 1)} \sum_{\lambda_1, L_1 M_1, \lambda_2, L_2 M_2, m_i, m_f} |D_{\lambda_2 L_2 M_2}^{\lambda_1 L_1 M_1}(E, \omega_1, \omega_2) \times (E, \omega_1, \omega_2) + D_{\lambda_1 L_1 M_1}^{\lambda_2 L_2 M_2}(E, \omega_2, \omega_1)|^2, \quad (5)$$

where

$$D_{\lambda_2 L_2 M_2}^{\lambda_1 L_1 M_1}(E, \omega_1, \omega_2) = \int d^3\mathbf{r}_1 d^3\mathbf{r}_2 \Psi_f^\dagger(\mathbf{r}_2) Q_{L_2 M_2}^{(\lambda_2)*}(\mathbf{r}_2, \omega_2) \times G_E(\mathbf{r}_2, \mathbf{r}_1) Q_{L_1 M_1}^{(\lambda_1)*}(\mathbf{r}_1, \omega_1) \Psi_i(\mathbf{r}_1), \quad (6)$$

$$Q_{L_j M_j}^{(\lambda_j)*}(\mathbf{r}_j, \omega_j) = \begin{cases} \boldsymbol{\alpha} \cdot \mathbf{A}_{L_j M_j}^{(0)*}(\mathbf{r}_j, \omega_j), & \lambda_j = 0, \\ \boldsymbol{\alpha} \cdot \mathbf{A}_{L_j M_j}^{(1)*}(\mathbf{r}_j, \omega_j) - G \Phi_{L_j M_j}^*(\mathbf{r}_j, \omega_j), & \lambda_j = 1. \end{cases} \quad (7)$$

It is understood that here and thereafter, $\omega_2 = E_i - E_f - \omega_1$. L, M stand for the photon angular momentum and its projection. $\boldsymbol{\alpha}$ are Dirac matrices and G is an arbitrary gauge parameter. $\Phi_{LM}(\mathbf{r})$ is the scalar potential and $\mathbf{A}_{LM}^{(0)}(\mathbf{r}), \mathbf{A}_{LM}^{(1)}(\mathbf{r})$ are the magnetic and electric vector potentials. Each of these multipoles can be expressed in terms of the spherical Bessel functions $j_L(\omega r)$ and the vector spherical harmonics $\mathbf{Y}_{L,\ell,M}(\hat{\mathbf{r}})$, $\ell = L, L \pm 1$ as defined by Akhiezer and Berestetskii [83],

$$\Phi_{LM}(\mathbf{r}, \omega) = i^L 4\pi j_L(\omega r) Y_{LM}(\hat{\mathbf{r}}), \quad (8)$$

$$\mathbf{A}_{LM}^{(0)}(\mathbf{r}, \omega) = i^L 4\pi j_L(\omega r) \mathbf{Y}_{L,L,M}(\hat{\mathbf{r}}), \quad (9)$$

$$\tilde{\mathbf{A}}_{LM}^{(1)}(\mathbf{r}, \omega) = i^{L+1} 4\pi \left\{ \sqrt{\frac{L}{2L+1}} j_{L+1}(\omega r) \mathbf{Y}_{L,L+1,M}(\hat{\mathbf{r}}) - \sqrt{\frac{L+1}{2L+1}} j_{L-1}(\omega r) \mathbf{Y}_{L,L-1,M}(\hat{\mathbf{r}}) \right\}, \quad (10)$$

$$\tilde{\mathbf{A}}_{LM}^{(-1)}(\mathbf{r}, \omega) = -i^{L+1} 4\pi \left\{ \sqrt{\frac{L+1}{2L+1}} j_{L+1}(\omega r) \mathbf{Y}_{L,L+1,M}(\hat{\mathbf{r}}) + \sqrt{\frac{L}{2L+1}} j_{L-1}(\omega r) \mathbf{Y}_{L,L-1,M}(\hat{\mathbf{r}}) \right\}. \quad (11)$$

In the above equations, $\hat{\mathbf{r}}$ is the unit vector along the three-dimensional space vector \mathbf{r} .

Let us focus our attention on the calculation of the D coefficients in Eqs. (6). Using the analytical expressions of the aforementioned bispinors and Dirac-Coulomb Green function, one easily obtains

$$D_{\lambda_2 L_2 M_2}^{\lambda_1 L_1 M_1}(E, \omega_1, \omega_2) = \sum_{n, \kappa, m} \langle f | Q_{L_1 M_1}^{(\lambda_1)*}(\omega_1) | n, \kappa, m \rangle \langle \widetilde{n, \kappa, m} | Q_{L_2 M_2}^{(\lambda_2)*}(\omega_2) | i \rangle, \quad (12)$$

where we set

$$\langle \mathbf{r} | i \rangle \equiv \Psi_i(\mathbf{r}) = \frac{1}{r} \left(i \frac{P_{n_i \kappa_i}(r) \Omega_{\kappa_i m_i}(\hat{\mathbf{r}})}{Q_{n_i \kappa_i}(r) \Omega_{-\kappa_i m_i}(\hat{\mathbf{r}})} \right), \quad (13)$$

$$\langle \mathbf{r} | f \rangle \equiv \Psi_f(\mathbf{r}) = \frac{1}{r} \left(i \frac{P_{n_f \kappa_f}(r) \Omega_{\kappa_f m_f}(\hat{\mathbf{r}})}{Q_{n_f \kappa_f}(r) \Omega_{-\kappa_f m_f}(\hat{\mathbf{r}})} \right),$$

$$\langle \mathbf{r} | n, \kappa, m \rangle = \frac{1}{r} \left(i \frac{S_{n\kappa}(2\lambda r) \Omega_{\kappa m}(\hat{\mathbf{r}})}{T_{n\kappa}(2\lambda r) \Omega_{-\kappa m}(\hat{\mathbf{r}})} \right), \quad (14)$$

$$\langle \mathbf{r} | \widetilde{n, \kappa, m} \rangle = \frac{1}{r} \left(i \frac{\tilde{\theta}_{n\kappa} S_{n\kappa}(2\lambda r) \Omega_{\kappa m}(\hat{\mathbf{r}})}{\tilde{\alpha}_{n\kappa} T_{n\kappa}(2\lambda r) \Omega_{-\kappa m}(\hat{\mathbf{r}})} \right).$$

It should be noted that $\kappa = \epsilon(j + 1/2)$, $j = l - \epsilon/2 = \bar{l} + \epsilon/2$, $\epsilon = \pm 1$. $\Omega_{\pm \kappa m}(\hat{\mathbf{r}}) \equiv \Omega_{jl(\bar{l})m}(\hat{\mathbf{r}})$ are spherical spinor harmonics [84] normalized according to $\int d\Omega \Omega_{\kappa' m'}^\dagger \Omega_{\kappa m} = \delta_{\kappa' \kappa} \delta_{m' m}$, and the plus and minus signs refer to l and \bar{l} , respectively. The radial components $S_{n\kappa}(2\lambda r)$, $T_{n\kappa}(2\lambda r)$, $P_{n\kappa}(r)$, and $Q_{n\kappa}(r)$ and the quantities λ , $\tilde{\theta}_{n\kappa}$, and $\tilde{\alpha}_{n\kappa}$ are defined and given in Appendix A. These functions form a basis for the irreducible representation D^j of SO(3) for both signs of the Dirac quantum number κ . The sums over n, κ, m occurring in the Green function run over all possible values of these indices, i.e., all the accessible intermediate states labeled by these quantum numbers. The reduction to radial integrals of the matrix elements in Eq. (12) is outlined in Appendix B. Thus, using these general results, Eq. (5) takes the form

$$\frac{dW^{(R)}}{d\omega_1} = \frac{2\alpha^2 \omega_1 \omega_2}{\pi(2j_i + 1)} \sum_{\lambda_1, L_1, \lambda_2, L_2} \left\{ \sum_j \left[|B_j(2,1)|^2 + |B_j(1,2)|^2 + 2B_j(2,1) \sum_{j'} K_{jj'}(2,1) B_{j'}^*(1,2) \right] \right\}, \quad (15)$$

where

$$\begin{aligned} B_j(2,1) &= \Delta_j(2,1) \sum_{n=-\infty}^{\infty} \check{M}_{f,n}^{(\lambda_2,L_2)}(E,\omega_2) \hat{M}_{n,i}^{(\lambda_1,L_1)}(E,\omega_1), \\ B_j(1,2) &= B_j(2,1; 1 \leftrightarrow 2). \end{aligned} \quad (16)$$

Denoting $[a,b,\dots] = (2a+1)(2b+1)\dots$, coefficients Δ_j and $K_{jj'}$ have a simple form via $3j$ and $6j$ symbols,

$$\begin{aligned} \Delta_j(2,1) &= [j_f, j, j_f]^{1/2} \begin{pmatrix} j_f & L_2 & j \\ 1/2 & 0 & -1/2 \end{pmatrix} \\ &\times \begin{pmatrix} j & L_1 & j_i \\ 1/2 & 0 & -1/2 \end{pmatrix}, \end{aligned} \quad (17)$$

$$K_{jj'}(2,1) = (-1)^{L_1+L_2+1} [j, j']^{1/2} \begin{Bmatrix} j_f & j' & L_1 \\ j_i & j & L_2 \end{Bmatrix}. \quad (18)$$

Hereafter, the electric and magnetic radial integrals may be written in closed form as follows:

$$\begin{aligned} \check{M}_{f,n}^{(1,L)}(E,\omega) &= \mathcal{F}_{f,n} - G(\mathcal{L}_{f,n} + \mathcal{H}_{f,n}), \\ \hat{M}_{n,i}^{(1,L)}(E,\omega) &= \mathcal{F}_{n,i} - G(\mathcal{L}_{n,i} + \mathcal{H}_{n,i}), \end{aligned} \quad (19)$$

$$\check{M}_{f,n}^{(0,L)}(E,\omega) = i\mathcal{T}_{f,n}, \quad \hat{M}_{n,i}^{(0,L)}(E,\omega) = i\mathcal{T}_{n,i}. \quad (20)$$

It should be noted that in Ref. [45], there is a misprint in Eq. (34), i.e., the corresponding direct term. The factor $1/[4\pi(2j_n+1)]$ should be replaced with $1/\sqrt{2j_n+1}$.

The issue of gauge invariance of matrix elements in multipole expansions has been discussed in great detail by Grant [85]. He showed that there are two values of G which are of particular interest, namely, that they lead to the well-known length and momentum forms of the transition operators in the nonrelativistic limit. In the length gauge, $G = -\sqrt{(L+1)/L}$, so that the radial integrals reduce to the following expressions:

$$\begin{aligned} \check{M}_{f,n}^{(1,L)}(E,\omega) &= \sqrt{\frac{2L+1}{L(L+1)}} [(L+1)\check{J}_L + (\kappa_f - \kappa)\check{I}_{L+1}^+ \\ &+ (L+1)\check{I}_{L+1}^-], \end{aligned} \quad (21)$$

$$\begin{aligned} \hat{M}_{n,i}^{(1,L)}(E,\omega) &= \sqrt{\frac{2L+1}{L(L+1)}} [(L+1)\hat{J}_L + (\kappa - \kappa_i)\hat{I}_{L+1}^+ \\ &+ (L+1)\hat{I}_{L+1}^-]. \end{aligned} \quad (22)$$

After some algebraic manipulations, Eqs. (21) and (22) can be conveniently cast into another form suitable for computations,

$$\begin{aligned} \check{M}_{f,n}^{(1,L)} &= \sqrt{\frac{2L+1}{L(L+1)}} \{ (L+1)[K_5(L,\omega) + K_6(L,\omega)] \\ &+ (\kappa_f - \kappa + L+1)K_3(L+1,\omega) \\ &+ (\kappa_f - \kappa - L-1)K_4(L+1,\omega) \}, \end{aligned} \quad (23)$$

$$\begin{aligned} \hat{M}_{n,i}^{(1,L)}(E,\omega) &= \sqrt{\frac{2L+1}{L(L+1)}} \{ \tilde{\theta}_{n\kappa}[(L+1)K_7(L,\omega) + (\kappa - \kappa_i \\ &+ L+1)K_1(L+1,\omega)] + \tilde{\alpha}_{n\kappa}[(L+1)K_8(L,\omega) \\ &+ (\kappa - \kappa_i - L-1)K_2(L+1,\omega)] \}. \end{aligned} \quad (24)$$

The following notations are used in Eqs. (23) and (24):

$$K_1(L,\omega) = \int_0^\infty dr Q_{n_i\kappa_i}(r) j_L(\omega r) S_{n\kappa}(2\lambda r), \quad (25)$$

$$K_2(L,\omega) = \int_0^\infty dr P_{n_i\kappa_i}(r) j_L(\omega r) T_{n\kappa}(2\lambda r), \quad (26)$$

$$K_3(L,\omega) = \int_0^\infty dr P_{n_f\kappa_f}(r) j_L(\omega r) T_{n\kappa}(2\lambda r), \quad (27)$$

$$K_4(L,\omega) = \int_0^\infty dr Q_{n_f\kappa_f}(r) j_L(\omega r) S_{n\kappa}(2\lambda r), \quad (28)$$

$$K_5(L,\omega) = \int_0^\infty dr P_{n_f\kappa_f}(r) j_L(\omega r) S_{n\kappa}(2\lambda r), \quad (29)$$

$$K_6(L,\omega) = \int_0^\infty dr Q_{n_f\kappa_f}(r) j_L(\omega r) T_{n\kappa}(2\lambda r), \quad (30)$$

$$K_7(L,\omega) = \int_0^\infty dr P_{n_i\kappa_i}(r) j_L(\omega r) S_{n\kappa}(2\lambda r), \quad (31)$$

$$K_8(L,\omega) = \int_0^\infty dr Q_{n_i\kappa_i}(r) j_L(\omega r) T_{n\kappa}(2\lambda r), \quad (32)$$

where $j_L(x)$ is the spherical Bessel function of the first kind. The second choice, i.e., the velocity gauge $G = 0$, leads to relations

$$\check{M}_{f,n}^{(1,L)}(E,\omega) = \frac{1}{\sqrt{L(L+1)(2L+1)}} \{ L[(\kappa_f - \kappa)\check{I}_{L+1}^+ + (L+1)\check{I}_{L-1}^-] - (L+1)[(\kappa_f - \kappa)\check{I}_{L-1}^+ - L\check{I}_{L-1}^-] \}, \quad (33)$$

$$\hat{M}_{n,i}^{(1,L)}(E,\omega) = \frac{1}{\sqrt{L(L+1)(2L+1)}} \{ L[(\kappa - \kappa_i)\hat{I}_{L+1}^+ + (L+1)\hat{I}_{L-1}^-] - (L+1)[(\kappa - \kappa_i)\hat{I}_{L-1}^+ - L\hat{I}_{L-1}^-] \}, \quad (34)$$

which may be rewritten in the form

$$\begin{aligned} \check{M}_{f,n}^{(1,L)}(E,\omega) &= \frac{1}{\sqrt{L(L+1)(2L+1)}} \{ L[(\kappa_f - \kappa + L+1)K_3(L+1,\omega) + (\kappa_f - \kappa - L-1)K_4(L+1,\omega)] \\ &- (L+1)[(\kappa_f - \kappa - L)K_3(L-1,\omega) + (\kappa_f - \kappa + L)K_4(L-1,\omega)] \}, \end{aligned} \quad (35)$$

$$\hat{M}_{n,i}^{(1,L)}(E,\omega) = \frac{1}{\sqrt{L(L+1)(2L+1)}} \{ \tilde{\theta}_{nk} [L(\kappa - \kappa_i + L + 1)K_1(L+1,\omega) - (L+1)(\kappa - \kappa_i - L)K_1(L-1,\omega)] \\ + \tilde{\alpha}_{nk} [L(\kappa - \kappa_i - L - 1)K_2(L+1,\omega) - (L+1)(\kappa - \kappa_i + L)K_2(L-1,\omega)] \}. \quad (36)$$

We also have, for magnetic-type multipoles,

$$\check{M}_{f,n}^{(0,L)}(E,\omega) = i\sqrt{\frac{2L+1}{L(L+1)}}(\kappa_f + \kappa)\check{I}_L^+, \quad \hat{M}_{n,i}^{(0,L)}(E,\omega) = i\sqrt{\frac{2L+1}{L(L+1)}}(\kappa + \kappa_i)\hat{I}_L^+, \quad (37)$$

i.e.,

$$\check{M}_{f,n}^{(0,L)}(E,\omega) = i\sqrt{\frac{2L+1}{L(L+1)}}(\kappa_f + \kappa)[K_3(L,\omega) + K_4(L,\omega)], \quad (38)$$

$$\hat{M}_{n,i}^{(0,L)}(E,\omega) = i\sqrt{\frac{2L+1}{L(L+1)}}(\kappa + \kappa_i)[\tilde{\theta}_{nk} K_1(L,\omega) + \tilde{\alpha}_{nk} K_2(L,\omega)]. \quad (39)$$

The K 's appearing in Eqs. (25)–(32) are Laplace-like integrals over products of spherical Bessel functions and generalized Laguerre polynomials and can be evaluated analytically. For the sake of brevity, we give here only the result for K_1 since the others can be treated analogously to it. By inserting $S_{nk}(2\lambda r)$ and $Q_{nk}(r)$ given by Eqs. (A5) and (A12), respectively, we get

$$K_1(L,\omega) = \frac{\sqrt{\pi}(x_i/2)^L \mathcal{F}_1}{2\Gamma(L+3/2)} \{ A_{nk} \tilde{C}_{n_i} \tilde{V}_L(\lambda, \lambda_i, \gamma, \gamma_i, n-1, n_i-1, 2\gamma, 2\gamma_i, x_i) - A_{nk} \tilde{D}_{n_i} \tilde{V}_L(\lambda, \lambda_i, \gamma, \gamma_i, n-1, n_i, 2\gamma, 2\gamma_i, x_i) \\ + B_{nk} \tilde{C}_{n_i} \tilde{V}_L(\lambda, \lambda_i, \gamma, \gamma_i, n, n_i-1, 2\gamma, 2\gamma_i, x_i) - B_{nk} \tilde{D}_{n_i} \tilde{V}_L(\lambda, \lambda_i, \gamma, \gamma_i, n, n_i, 2\gamma, 2\gamma_i, x_i) \}, \quad (40)$$

where we set

$$\tilde{V}_L(\lambda, \lambda_i, \gamma, \gamma_i, m, n, \alpha, \beta, x_i) = \mathcal{Y}^\gamma \mathcal{Y}_i^{\gamma_i} \Gamma(m+\alpha+1)\Gamma(n+\beta+1) \sum_{p=0}^m \frac{(-\mathcal{Y})^p}{\Gamma(p+1)\Gamma(p+\alpha+1)\Gamma(m-p+1)} \\ \times \sum_{q=0}^n \frac{(-\mathcal{Y}_i)^q \Gamma(s_i) {}_2F_1(s_i/2, (s_i+1)/2; L+3/2; -x_i^2)}{\Gamma(q+1)\Gamma(q+\beta+1)\Gamma(n-q+1)}, \quad (41)$$

$$\mathcal{Y}_i = 2\lambda_i \mathcal{F}_i, \quad \mathcal{Y} = 2\lambda \mathcal{F}_i, \quad \mathcal{F}_i = 1/(\lambda + \lambda_i), \quad s_i = \gamma + \gamma_i + p + q + L + 1, \quad x_i = \omega \mathcal{F}_i.$$

Another method of calculation of K_1 is based on the insertion of the expansion of the spherical Bessel function in the Taylor series [86],

$$j_L(\omega r) = \sum_{v=0}^{\infty} \frac{(-1)^v}{2^v v! (2L+2v+1)!!} (\omega r)^{2v+L}, \quad (42)$$

into the integral (25). As should be expected intuitively, the analytic expression obtained matches Eq. (40) in which Gauss hypergeometric functions ${}_2F_1(a,b;c;x)$ have been expanded in Eq. (41). This is indeed the case, considering, for instance, successively the first $v=0$ and the second $v=1$ contributions in the latter summation that lead exactly to Eqs. (40) and (41) in which ${}_2F_1(a,b;c;x)$ is substituted by 1 and $(ab/c)x$, respectively. Since the truncation of Eq. (42) is so much simpler than the fully relativistic calculation, it is of interest to determine its limits of validity. We will address this problem of retardation in the transition operator in Sec. IV.

B. Application to some transition probabilities for $2s_{1/2}$ and $2p_{1/2}$ states

In connection with the next section, it is interesting to give, in what follows, closed forms of Eq. (15) for the two-photon

processes $2s_{1/2} \rightarrow 1s_{1/2} + 2\gamma(E1)$, $2s_{1/2} \rightarrow 1s_{1/2} + 2\gamma(E2)$, and $2p_{1/2} \rightarrow 1s_{1/2} + \gamma(E1) + \gamma(E2)$. In the nonrelativistic limit, they recover the expressions derived in the next section. In order to present the spectral frequency, Eq. (15) may be rewritten in the form

$$\frac{dW^{(R)}}{dy} = \frac{\alpha^2 y(1-y)\omega_0^3}{\pi} Q, \quad \omega_1 = \omega_0 y, \\ \omega_2 = \omega_0(1-y), \quad \omega_0 = E_i - E_f, \quad 0 < y < 1, \quad (43)$$

where y is the fraction of energy carried by one of the two photons, and ω_0 is the energy of the two-photon transition. The Dirac energies E_i and E_f of the initial and final states are given by Eq. (A15). After somewhat lengthy calculations, we find, for the $2E1$ decay,

$$Q^{(2E1)} = 2\{[A^{(2E1)}(2,1; p_{1/2})]^2 + [A^{(2E1)}(1,2; p_{1/2})]^2\} \\ + 4\{[A^{(2E1)}(2,1; p_{3/2})]^2 + [A^{(2E1)}(1,2; p_{3/2})]^2\} \\ + \frac{4}{3}[-A^{(2E1)}(2,1; p_{1/2})A^{(2E1)}(1,2; p_{1/2}) \\ + 4A^{(2E1)}(2,1; p_{1/2})A^{(2E1)}(1,2; p_{3/2}) \\ + 4A^{(2E1)}(2,1; p_{3/2})A^{(2E1)}(1,2; p_{1/2}) \\ + 2A^{(2E1)}(2,1; p_{3/2})A^{(2E1)}(1,2; p_{3/2})], \quad (44)$$

where

$$\begin{aligned} & A^{(2E1)}(2,1; p_{1/2}) \\ &= 2 \sum_{n=-\infty}^{\infty} \{K_5(1,\omega_2) + K_6(1,\omega_2) - 2K_4(2,\omega_2)\} \\ &\quad \times \{\tilde{\theta}_{nk}[K_7(1,\omega_1) + 2K_1(2,\omega_1)] + \tilde{\alpha}_{nk}K_8(1,\omega_1)\}, \quad (45) \end{aligned}$$

$$\begin{aligned} & A^{(2E1)}(2,1; p_{3/2}) \\ &= \frac{1}{2} \sum_{n=-\infty}^{\infty} \{2(K_5(1,\omega_2) + K_6(1,\omega_2)) + 3K_3(2,\omega_2) \\ &\quad - K_4(2,\omega_2)\} \{\tilde{\theta}_{nk}[2K_7(1,\omega_1) + K_1(2,\omega_1)] \\ &\quad + \tilde{\alpha}_{nk}[2K_8(1,\omega_1) - 3K_2(2,\omega_1)]\}, \quad (46) \end{aligned}$$

$$A^{(2E1)}(1,2; p_{1/2}) = A^{(2E1)}(2,1; p_{1/2}; \omega_2 \leftrightarrow \omega_1), \quad (47)$$

$$A^{(2E1)}(1,2; p_{3/2}) = A^{(2E1)}(2,1; p_{3/2}; \omega_2 \leftrightarrow \omega_1). \quad (48)$$

In a similar manner, we have the desired relations for the two other decay channels,

$$\begin{aligned} Q^{(2E2)} &= 4\{[A^{(2E2)}(2,1; d_{3/2})]^2 + [A^{(2E2)}(1,2; d_{3/2})]^2\} \\ &\quad + 6\{[A^{(2E2)}(2,1; d_{5/2})]^2 + [A^{(2E2)}(1,2; d_{5/2})]^2\} \\ &\quad + \frac{4}{5}\{-2A^{(2E2)}(2,1; d_{3/2})A^{(2E2)}(1,2; d_{3/2}) \\ &\quad + 12A^{(2E2)}(2,1; d_{3/2})A^{(2E2)}(1,2; d_{5/2}) \\ &\quad + 12A^{(2E2)}(2,1; d_{5/2})A^{(2E2)}(1,2; d_{3/2}) \\ &\quad + 3A^{(2E2)}(2,1; d_{5/2})A^{(2E2)}(1,2; d_{5/2})\}, \quad (49) \end{aligned}$$

with

$$\begin{aligned} & A^{(2E2)}(2,1; d_{3/2}) \\ &= \frac{3}{2} \sum_{n=-\infty}^{\infty} \{K_5(2,\omega_2) + K_6(2,\omega_2) - 2K_4(3,\omega_2)\} \\ &\quad \times \{\tilde{\theta}_{nk}[K_7(2,\omega_1) + 2K_1(3,\omega_1)] + \tilde{\alpha}_{nk}K_8(2,\omega_1)\}, \quad (50) \end{aligned}$$

$$\begin{aligned} & A^{(2E2)}(2,1; d_{5/2}) \\ &= \frac{1}{6} \sum_{n=-\infty}^{\infty} \{3[K_5(2,\omega_2) + K_6(2,\omega_2)] + 5K_3(3,\omega_2) \\ &\quad - K_4(3,\omega_2)\} \{\tilde{\theta}_{nk}[3K_7(2,\omega_1) + K_1(3,\omega_1)] \\ &\quad + \tilde{\alpha}_{nk}[3K_8(2,\omega_1) - 5K_2(3,\omega_1)]\}, \quad (51) \end{aligned}$$

$$A^{(2E2)}(1,2; d_{3/2}) = A^{(2E2)}(2,1; d_{3/2}; \omega_2 \leftrightarrow \omega_1), \quad (52)$$

$$A^{(2E2)}(1,2; d_{5/2}) = A^{(2E2)}(2,1; d_{5/2}; \omega_2 \leftrightarrow \omega_1), \quad (53)$$

and

$$\begin{aligned} & Q^{(E1E2)} = [A^{(E2,E1)}(2,1; d_{3/2}) + A^{(E1,E2)}(1,2; p_{3/2})]^2 \\ &\quad + [A^{(E1,E2)}(2,1; p_{3/2}) + A^{(E2,E1)}(1,2; d_{3/2})]^2, \quad (54) \end{aligned}$$

$$\begin{aligned} & A^{(E2,E1)}(2,1; d_{3/2}) \\ &= \sqrt{3} \sum_{n=-\infty}^{\infty} \{K_5(2,\omega_2) + K_6(2,\omega_2) - 2K_4(3,\omega_2)\} \\ &\quad \times \{\tilde{\theta}_{nk}[3K_1(2,\omega_1) + 2K_7(1,\omega_1)] \\ &\quad + \tilde{\alpha}_{nk}[2K_8(1,\omega_1) - K_2(2,\omega_1)]\}, \quad (55) \end{aligned}$$

$$\begin{aligned} & A^{(E1,E2)}(1,2; p_{3/2}) = \sqrt{3} \sum_{n=-\infty}^{\infty} \{2(K_5(1,\omega_1) + K_6(1,\omega_1)) \\ &\quad + 3K_3(2,\omega_1) - K_4(2,\omega_1)\} \{\tilde{\theta}_{nk}K_7(2,\omega_2) \\ &\quad + \tilde{\alpha}_{nk}[K_8(2,\omega_2) - 2K_2(3,\omega_2)]\}, \quad (56) \end{aligned}$$

$$A^{(E2,E1)}(1,2; d_{3/2}) = A^{(E2,E1)}(2,1; d_{3/2}; \omega_2 \leftrightarrow \omega_1), \quad (57)$$

$$A^{(E1,E2)}(2,1; p_{3/2}) = A^{(E1,E2)}(1,2; p_{3/2}; \omega_1 \leftrightarrow \omega_2). \quad (58)$$

III. NONRELATIVISTIC TREATMENT

First of all, it should be pointed out that some formulas given in Ref. [35] for two electric-photon transitions in hydrogen are incorrect, such as Eqs. (26), (31), (37), (39), (41), (44), and (45). However, it should also be emphasized that some of them have been corrected by Solovyev *et al.* [36]. Hence, in this section, we derive corresponding relations which, as may be verified, are the nonrelativistic limits of the results obtained in the above relativistic formalism. For a nonrelativistic hydrogenic system, the following two electric-photon decay rate in a.u. needs to be evaluated:

$$\begin{aligned} d^2W^{(NR)} &= \frac{2\pi\alpha^2}{2l_i+1} \left(\sum_{L_1M_1, L_2M_2, m_i, m_f} |\mathcal{U}_{fi}^{(1)} + \mathcal{U}_{fi}^{(2)}|^2 \right) \\ &\quad \times \delta(\xi_i - \xi_f - \omega_1 - \omega_2) \frac{Rd\omega_2}{\pi} \frac{Rd\omega_1}{\pi}, \quad (59) \end{aligned}$$

$$\begin{aligned} \mathcal{U}_{fi}^{(1)} &= \int d^3\mathbf{r}_1 d^3\mathbf{r}_2 \psi_f^*(\mathbf{r}_2) \tilde{V}_{L_2M_2}(\mathbf{r}_2, \omega_2) \\ &\quad \times G_\xi(\mathbf{r}_2, \mathbf{r}_1) \tilde{V}_{L_1M_1}(\mathbf{r}_1, \omega_1) \psi_i(\mathbf{r}_1), \quad (60) \end{aligned}$$

$$\begin{aligned} \mathcal{U}_{fi}^{(2)} &= \int d^3\mathbf{r}_1 d^3\mathbf{r}_2 \psi_f^*(\mathbf{r}_2) \tilde{V}_{L_1M_1}(\mathbf{r}_2, \omega_1) \\ &\quad \times G_\xi(\mathbf{r}_2, \mathbf{r}_1) \tilde{V}_{L_2M_2}(\mathbf{r}_1, \omega_2) \psi_i(\mathbf{r}_1), \quad (61) \end{aligned}$$

where R is the radius of the normalizing sphere. ξ_i and ξ_f are the nonrelativistic binding energies of the initial and final states, respectively, as defined in Eq. (A19) in Appendix A. Notice that on one hand, the emission of the electric photon EL is described by the potentials [83]

$$\tilde{V}_{LM}(\mathbf{r}, \omega) = (-i)^L \left(\frac{4\pi\omega}{R} \right)^{1/2} \sqrt{\frac{L+1}{L}} \frac{(\alpha\omega)^L}{(2L+1)!!} r^L Y_{lm}^*(\hat{\mathbf{r}}), \quad (62)$$

and, on the other hand, the Green function is given in Appendix A. After performing the angular reduction in

Eqs. (60) and (61), we find

$$\mathcal{U}_{fi}^{(1)} = \frac{1}{R} \frac{\alpha^{L_1+L_2} \omega_1^{L_1+1/2} \omega_2^{L_2+1/2}}{(2L_1+1)!! (2L_2+1)!!} \sqrt{\frac{(L_1+1)(L_2+1)[L_1, L_2]}{L_1 L_2}} Q(2,1), \quad (63)$$

$$Q(2,1) = \sum_l q_l(2,1) \theta_l(2,1), \quad q_l(2,1) = \Delta_l(2,1) I_l(\xi; 2,1), \quad (64)$$

$$I_l(\xi; 2,1) = \int_0^\infty dr_2 dr_1 r_2^{L_2} r_1^{L_1} P_f(r_2) g_l(\xi; r_2, r_1) P_i(r_1), \quad (65)$$

$$\Delta_l(2,1) = [l_f, l, l_i]^{1/2} \begin{pmatrix} l_f & L_1 & l \\ 0 & 0 & 0 \end{pmatrix} \begin{pmatrix} l & L_2 & l_i \\ 0 & 0 & 0 \end{pmatrix} \Pi(l_f, l, l_i, L_1, L_2), \quad (66)$$

$$\theta_l(2,1) = [l]^{1/2} \sum_m (-1)^{m+m_i} \begin{pmatrix} l_f & L_2 & l \\ -m_f & -M_2 & m \end{pmatrix} \begin{pmatrix} l & L_1 & l_i \\ -m & -M_1 & m_i \end{pmatrix}, \quad (67)$$

with $\Pi(l_f, l, l_i, L_1, L_2) = 1$ if $l_f + l + L_1$ and $l_i + l + L_2$ are even numbers, and $\Pi(l_f, l, l_i, L_1, L_2) = 0$ otherwise. Note also that

$$\mathcal{U}_{fi}^{(2)} = \mathcal{U}_{fi}^{(1)} (2 \leftrightarrow 1). \quad (68)$$

Further, on substituting the relations (63)–(68) into Eq. (59) and integrating over ω_2 , we have

$$\frac{dW^{(NR)}}{d\omega_1} = \frac{2\pi}{2l_i+1} \sum_{L_1, L_2} \alpha^{2(L_1+L_2+1)} \zeta_{L_1, L_2} \omega_1^{L_1+1/2} \omega_2^{L_2+1/2} \left\{ \sum_{M_1, M_2, m_i, m_f} |Q(2,1) + Q(1,2)|^2 \right\}, \quad (69)$$

$$\zeta_{L_1, L_2} = \frac{(L_1+1)(L_2+1)[L_1, L_2]}{L_1 L_2 [(2L_1+1)!! (2L_2+1)!!]^2}, \quad (70)$$

and now $\omega_2 = \xi_i - \xi_f - \omega_1$. Hence, applying the same method as in the relativistic case, i.e., using the well-known sum rules for θ_l , finally yields

$$\frac{dW^{(NR)}}{d\omega_1} = \frac{2}{\pi (2l_i+1)} \sum_{L_1, L_2} \alpha^{2(L_1+L_2+1)} \zeta(L_1, L_2) \omega_1^{2L_1+1} \omega_2^{2L_2+1} \sum_l \left[|q_l(2,1)|^2 + |q_l(1,2)|^2 + 2q_l(2,1) \sum_{l'} K_{ll'}(2,1) q_{l'}(1,2) \right], \quad (71)$$

$$K_{ll'}(2,1) = (-1)^{L_1+L_2+1} [l, l']^{1/2} \begin{Bmatrix} l_f & l' & L_1 \\ l_i & l & L_2 \end{Bmatrix}. \quad (72)$$

The radial integral in Eq. (65) can be evaluated analytically by using the formula

$$\begin{aligned} D_l(m; p, q, ; \lambda) &= Z^m \int_0^\infty dr_2 dr_1 e^{-Z(r_2+(r_1/2))} r_2^p r_1^q g_l(\xi; r_2, r_1) \\ &= \frac{2^{3l+q+4} \nu^{p+q+3}}{(\nu+1)^{l+p+2} (\nu+2)^{l+q+2} Z^{p+q-m+3}} \frac{(l+p+1)! (l+q+1)!}{[(2l+1)!]^2} \\ &\times \sum_{n=0}^\infty \frac{(n+2l+1)!}{(n+l+1-\nu) n!} {}_2F_1 \left(-n, l+p+2; 2l+2; \frac{2}{\nu+1} \right) {}_2F_1 \left(-n, l+q+2; 2l+2; \frac{4}{\nu+2} \right), \\ &\nu = \lambda/Z, \quad \lambda = \sqrt{-2E}. \end{aligned} \quad (73)$$

Application of the above formulas to the $2s \rightarrow 1s + 2\gamma(E1)$, $2s \rightarrow 1s + 2\gamma(E2)$, and $2p \rightarrow 1s + \gamma(E1) + \gamma(E2)$ transitions gives, respectively, the following.

(i) $2E1$ frequency distribution for the $2s$ state.

$$\frac{dW^{(NR)}}{dy} = \frac{2^9 3^4}{\pi} (\alpha Z)^6 y^3 (1-y)^3 [\tilde{I}_1(\nu) + \tilde{I}_1(\nu')]^2, \quad (74)$$

$$\tilde{I}_1(\nu) = \frac{\nu^7}{(\nu+1)^5 (\nu+2)^5} \sum_{n=0}^\infty \frac{(n+3)!}{n! (n+2-\nu)} {}_2F_1 \left(-n, 5; 4; \frac{2}{\nu+1} \right) \left[{}_2F_1 \left(-n, 5; 4; \frac{4}{\nu+2} \right) - \frac{5\nu}{\nu+2} {}_2F_1 \left(-n, 6; 4; \frac{4}{\nu+2} \right) \right], \quad (75)$$

$$\nu = \frac{2}{\sqrt{1+3y}}, \quad \nu' = \frac{2}{\sqrt{4-3y}}, \quad \omega_0 = \xi_i - \xi_f, \quad \omega_1 = y\omega_0, \quad \omega_2 = (1-y)\omega_0, \quad 0 < y < 1. \quad (76)$$

Performing an integration over y , the emission probability reads $W^{(NR)}(2E1) = 1.318\,222\,666\,9 \times 10^{-3} (\alpha Z)^6$ a.u.

(ii) *2E2 frequency distribution for the 2s state.*

$$\begin{aligned} \frac{dW^{(NR)}}{dy} &= \frac{3^{13}}{2^3 5^3 \pi} (\alpha Z)^{10} y^5 (1-y)^5 [\tilde{I}_2(\nu) + \tilde{I}_2(\nu')]^2, \\ \tilde{I}_2(\nu) &= \frac{\nu^9}{(\nu+1)^7(\nu+2)^7} \sum_{n=0}^{\infty} \frac{(n+5)!}{(n+3-\nu)n!} {}_2F_1\left(-n, 7; 6; \frac{2}{\nu+1}\right) \left[{}_2F_1\left(-n, 7; 6; \frac{4}{\nu+2}\right) - \frac{7\nu}{\nu+2} {}_2F_1\left(-n, 8; 6; \frac{4}{\nu+2}\right) \right], \end{aligned} \quad (77)$$

and $W^{(NR)}(2E2) = 2.772\,078\,993\,3 \times 10^{-7} (\alpha Z)^{10}$ a.u.

(iii) *E1E2 frequency distribution for the 2p state.*

$$\frac{dW^{(NR)}}{dy} = \frac{2^4 3^7}{5^2 \pi} (\alpha Z)^8 y^3 (1-y)^3 \{ (1-y)^2 [\hat{I}_1(\nu') + \hat{I}_2(\nu)]^2 + y^2 [\hat{I}_1(\nu) + \hat{I}_2(\nu')]^2 \}, \quad (79)$$

$$\hat{I}_1(\nu) = \frac{10\nu^9}{(\nu+1)^7(\nu+2)^7} \sum_{n=0}^{\infty} \frac{(n+3)!}{(n+2-\nu)n!} {}_2F_1\left(-n, 5; 4; \frac{2}{\nu+1}\right) {}_2F_1\left(-n, 7; 4; \frac{4}{\nu+2}\right), \quad (80)$$

$$\hat{I}_2(\nu) = \frac{3\nu^9}{(\nu+1)^7(\nu+2)^7} \sum_{n=0}^{\infty} \frac{(n+5)!}{(n+3-\nu)n!} {}_2F_1\left(-n, 7; 6; \frac{2}{\nu+1}\right) {}_2F_1\left(-n, 7; 6; \frac{4}{\nu+2}\right), \quad (81)$$

and $W^{(NR)}(E1E2) = 1.988\,964\,910\,4 \times 10^{-5} (\alpha Z)^8$ a.u.

It may be shown without difficulty that relations (74)–(81) agree with the corresponding nonrelativistic limits of expressions (43)–(58) derived previously in the relativistic theory. Indeed, note that only K_5 and K_7 containing upper components $P_{nk}(r)$ of radial Dirac bispinors and $S_{nk}(2\lambda r)$ of the radial Sturmians must be considered together with non-negative values ($n \geq 0$) of the radial quantum number.

IV. NUMERICAL RESULTS AND DISCUSSION

For the sake of assessing the effectiveness of our DCGF approach, we apply in this section the formulas derived above to a large selection of hydrogenic ions with nuclear charge Z up to 100. Before presenting below the main numerical results and a comparison with other refined computations, some introductory statements are in order. First of all, we introduce the standard spectral distribution as suggested by Spitzer and Greenstein [29],

$$\frac{dW}{dy} = \frac{9}{2^{10}} \mathcal{Z}^q \psi(Z, y), \quad \mathcal{Z} = \alpha Z. \quad (82)$$

Here, α is the fine-structure constant. In the scaling factor, we have $q = 8$ for $E1M1$ and $E1E2$; $q = 12$ for $M1M2$ in the $2p_{1/2} \rightarrow 1s_{1/2}$ transition, while $q = 6$ for $2E1$; $q = 10$ for $E1M2$, $2M1$, and $2E2$; and $q = 14$ for $2M2$ and $E2M1$ in the $2s_{1/2} \rightarrow 1s_{1/2}$ transition. By integrating Eq. (82), we get the total rate [35,36,45]

$$W = \frac{1}{2} \int_0^1 \left(\frac{dW}{dy} \right) dy, \quad W = \mathcal{Z}^q \phi(Z). \quad (83)$$

Then, having derived our formulas in relativistic atomic units (r.a.u.) and atomic units (a.u.), it is worth noting the following

conversion relationships:

$$W^{(R)}(s^{-1}) = W^{(R)}(\text{r.a.u.})/\tau_0^{(R)}, \quad \tau_0^{(R)} = \alpha a_0/c, \quad (84)$$

$$W^{(NR)}(s^{-1}) = W^{(NR)}(\text{a.u.})/\tau_0^{(NR)}, \quad \tau_0^{(NR)} = a_0/(\alpha c), \quad (85)$$

$$\begin{aligned} W^{(R)}(\text{r.a.u.}) &= \alpha^2 W^{(R)}(\text{a.u.}), \\ W^{(R)}(s^{-1}) &= W^{(R)}(\text{a.u.})/\tau_0^{(NR)}, \end{aligned} \quad (86)$$

where, as mentioned previously, $\tau_0^{(NR)}$ and $\tau_0^{(R)}$ are the atomic and relativistic atomic units of time, respectively. Using values of physical constants given in Ref. [82], one obtains $\tau_0^{(R)} = 1.288\,088\,668 \times 10^{-21}$ s, $\tau_0^{(NR)} = 24.188\,843\,26 \times 10^{-18}$ s, with $\alpha^{-1} = 137.035\,999\,11$.

In the sums over the radial quantum number n occurring in equations of Secs. II and III, a finite expansion length n_{\max} has been considered to obtain converged values, so that the integrated two-photon decay rates $W^{(R)}$, $W_+^{(R)}$, $W_-^{(R)}$, and

TABLE I. Virtual states allowed in the multipole contributions included in calculations of two-photon decay rates for the $2s_{1/2} \rightarrow 1s_{1/2}$ and $2p_{1/2} \rightarrow 1s_{1/2}$ transitions.

$2s_{1/2} \rightarrow 1s_{1/2}$		$2p_{1/2} \rightarrow 1s_{1/2}$	
Multipoles	Virtual states	Multipoles	Virtual states
$2E1$	$p_{1/2}, p_{3/2}$	$E1E2$	$p_{3/2}, d_{3/2}$
$E1M2$	$p_{3/2}$	$E1M1$	$s_{1/2}, p_{1/2}, p_{3/2}, d_{3/2}$
$2M1$	$s_{1/2}, d_{3/2}$	$M1M2$	$s_{1/2}, d_{3/2}$
$2E2$	$d_{3/2}, d_{5/2}$		
$2M2$	$p_{3/2}, f_{5/2}$		
$E2M1$	$d_{3/2}$		

TABLE II. Predicted partial sums of the integrated decay rates $W^{(R)}$ (r.a.u.) of the $E1E2$ multipole contribution for the transition $2p_{1/2} \rightarrow 1s_{1/2}$ at nuclear charges $Z = 1, 30, 50$, and 100 . n_{\max} denotes the highest radial quantum number considered in the Sturmian basis. The numbers in parentheses indicate the powers of 10 by which the values are to be multiplied.

n_{\max}	Z			
	1	30	50	100
1	9.3861914602(-27)	5.9512415506(-15)	3.3240368982(-13)	5.8151021591(-11)
5	8.5165466456(-27)	5.4133587740(-15)	3.0378665646(-13)	5.4659701315(-11)
8	8.5165816233(-27)	5.4133544536(-15)	3.0378324501(-13)	5.4655745883(-11)
10	8.5165816161(-27)	5.4133548047(-15)	3.0378331550(-13)	5.4655757211(-11)
20	8.5165816161(-27)	5.4133551830(-15)	3.0378334029(-13)	5.4655758861(-11)
30	8.5165816161(-27)	5.4133551830(-15)	3.0378334029(-13)	5.4655758863(-11)

$W^{(NR)}$ generate fully relativistic results, contributions of the non-negative and negative parts of the Sturmians spectrum, and nonrelativistic numbers, respectively. Notice that they have been computed from Eq. (83) by using a Gauss-Legendre quadrature.

Finally, let

$$d(\%) = 100 \times \frac{|W^{(R)} - W^{(\text{app})}|}{W^{(R)}} \quad (87)$$

be a measure of the difference between our fully relativistic results $W^{(R)}$ considered as reference numbers and other theoretical data $W^{(\text{app})} \equiv W_+^{(R)}, W_-^{(R)}, W^{(NR)}$ [this work, Eqs. (74)–(81)], $W^{(GD)}$ (Ref. [41]), $W^{(L)}$ (Ref. [45]), $W^{(S)}$ (Ref. [44]), $W^{(A)}$ (Ref. [47]), and $W^{(PJ)}$ (Ref. [43]). Now we are ready to apply these expressions for studying two-photon decay rates of the two selected $2s_{1/2}$ and $2p_{1/2}$ atomic states.

In Table I, we present the list of multipoles included in our calculations and, in each case, the allowed virtual states in the summation of Eq. (15). Notice that the term $f_{5/2}$ has not been taken into account in Ref. [41]. In Tables II and III, the convergence of the summation over n is shown for two multipole decay channels $E1E2$ and $2E1$, respectively. It clearly appears at inspection that the convergence of the series expansion is somewhat slow when the nuclear charge increases, and no more than about 30 terms are needed to reach the stability and accuracy to eight digits. It is important to underline at this point that unless great care is exercised, the evaluation of radial integrals (25)–(32) involved in matrix elements can lead to erroneous conclusions. Once these most crucial quantities are determined, the task of obtaining differential as well as total transition rates becomes fairly straightforward. We have proceeded efficiently, on one hand, by making use of a Gauss-Laguerre quadrature well adapted to Eqs. (25)–(32)

and, on the other hand, by employing for Eq. (41) the computer-algebra code MAPLE to avoid roundoff errors. We have checked that both estimates are in exact agreement up to at least eight significant digits, and obtained very accurate numerical values of radial integrals. The basis parameter used in the calculation of our results in this paper is $n_{\max} = 30$. Moreover, we have also studied the gauge invariance of our decay-rate numbers, except multipoles with only magnetic components which are only defined in the velocity gauge. As expected from the well-known general requirement of gauge invariance, they are practically independent of G , namely, the relativistic counterparts of the length and velocity forms yield almost identical results (i.e., with a relative difference less than 10^{-10}) for all multipole decay channels.

We display in Tables IV–VII the Z dependence of detailed calculations for the $2p_{1/2} \rightarrow 1s_{1/2}$ and $2s_{1/2} \rightarrow 1s_{1/2}$ transitions. The breakdown of integrated decay rates into contributions from different combinations of multipoles is shown. Our results are compared with predictions of other authors. In order to illustrate how closely our computations agree with these values and to be more informative, we have plotted in Figs. 1–4 the percentage difference d as a function of the nuclear charge. When cross examining these figures together with the tables, a few relevant features become apparent, including the following.

(a) The magnitude of d lies between 0.1–1.4% for W^L ($E1M1, E1E2$) values, computed for the first time by Labzowsky *et al.* [45], and, apart from $E2M1$, under 0.03% for W^{GD} [41] and W^{PJ} ($2E1$) [43]. Notice that the percentage difference for W^L ($2E1$), which is about 0.1%, is not represented in Fig. 2. Thus, the results from Goldman and Drake [41] are closer to those of this work, with, however, a marked divergence (26–43%) for multipoles with only

TABLE III. Same as Table II for the $2E1$ multipole contribution of the transition $2s_{1/2} \rightarrow 1s_{1/2}$.

n_{\max}	Z			
	1	30	50	100
1	1.0821906345(-20)	7.6265691549(-12)	1.5433574477(-10)	7.4379370598(-9)
5	1.0599509837(-20)	7.4979889968(-12)	1.5285087794(-10)	7.7046978633(-9)
8	1.0599760340(-20)	7.4981326509(-12)	1.5285262701(-10)	7.7046053190(-9)
10	1.0599760295(-20)	7.4981327091(-12)	1.5285263188(-10)	7.7046041375(-9)
20	1.0599760295(-20)	7.4981331007(-12)	1.5285263991(-10)	7.7046041295(-9)
30	1.0599760295(-20)	7.4981331007(-12)	1.5285263991(-10)	7.7046041186(-9)

TABLE IV. Contributions from different combinations of multipoles to the integrated two-photon decay rates $W(s^{-1})$ for the transition $2p_{1/2} \rightarrow 1s_{1/2}$ as a function of the nuclear charge. First entry: $W^{(R)}$; second entry: $W_+^{(R)}$; third entry: $W_-^{(R)}$; fourth entry: $W^{(So)}$ (Solov'yev *et al.* [36], Labzowsky *et al.* [35]); fifth entry: $W^{(NR)}$ [Eqs. (79)–(81)]; sixth entry: $W^{(L)}$ (Labzowsky *et al.* [45]). Powers of ten are given in parentheses.

Z	$W(E1M1)$	$W(E1E2)$	$W(M1M2)$
1	9.676656(−6)	6.611798(−6)	3.827879(−17)
	1.630764(−5)	6.611777(−6)	3.159442(−17)
	1.002436(−6)	1.826741(−17)	6.835281(−18)
	9.67696(−6)	6.61201(−6)	
		6.612027(−6)	
	9.667(−6)	6.604(−6)	
	9.646776(2)	6.589077(2)	3.790688(−5)
	1.624728(3)	6.586974(2)	3.124388(−5)
	9.993125(1)	1.828967(−5)	6.850695(−6)
	9.67696(2)	6.61201(2)	
10		6.612027(2)	
	9.637(2)	6.582(2)	
	2.446386(5)	1.669178(5)	1.510057(−1)
	4.112301(5)	1.667031(5)	1.239768(−1)
	2.533893(4)	7.519083(−2)	2.825470(−2)
	2.47730(5)	1.69267(5)	
		1.692679(5)	
	2.443(5)	1.667(5)	
	6.171112(6)	4.202626(6)	1.876852(1)
	1.033754(7)	4.190309(6)	1.531755(1)
20	6.389113(5)	9.815447(0)	3.709259(0)
	6.34905(6)	4.33814(6)	
		4.338151(6)	
	6.164(6)	4.198(6)	
	6.027546(7)	4.092510(7)	5.603699(2)
	1.004201(8)	4.070804(7)	4.538585(2)
	6.233007(6)	3.125000(2)	1.191049(2)
	6.34189(7)	4.33325(7)	
		4.333258(7)	
	6.021(7)	4.088(7)	
50	3.490198(8)	2.358404(8)	7.626644(3)
	5.766927(8)	2.338399(8)	6.121721(3)
	3.598843(7)	4.596473(3)	1.773218(3)
	3.78006(8)	2.58282(8)	
		2.582823(8)	
	3.486(8)	2.355(8)	
	1.448849(9)	9.713598(8)	6.295649(4)
	2.364553(9)	9.591454(8)	5.002899(4)
	1.484800(8)	4.151041(4)	1.628368(4)
	1.62536(9)	1.11056(9)	
70		1.110567(9)	
	4.775562(9)	3.159314(9)	3.670109(5)
	7.650156(9)	3.103292(9)	2.885631(5)
	4.834404(8)	2.678235(5)	1.074857(5)
	5.57857(9)	3.81169(9)	
		3.811702(9)	
	4.767(9)	3.152(9)	
	1.330702(10)	8.600491(9)	1.653622(6)
	2.072144(10)	8.392647(9)	1.286627(6)
	1.315901(9)	1.350922(6)	5.592928(5)

TABLE IV. (Continued.)

Z	$W(E1M1)$	$W(E1E2)$	$W(M1M2)$
90	1.62352(10)	1.10931(10)	
		1.109314(10)	
	1.328(10)	8.569(9)	
	3.275569(10)	2.030312(10)	6.096777(6)
	4.882438(10)	1.964975(10)	4.702271(6)
	3.100586(9)	5.642668(6)	2.438090(6)
	4.16561(10)	2.84625(10)	
		2.846261(10)	
	3.262(10)	2.016(10)	
	7.391723(10)	4.243167(10)	1.908566(7)
100	1.029402(11)	4.063967(10)	1.466435(7)
		6.453893(9)	9.299941(6)
	9.67696(10)	6.61201(10)	
		6.612027(10)	
	7.330(10)	4.187(10)	

magnetic components, i.e., $2M2$ and $2M1$. In Table V are also compiled a few numerical values from Amaro *et al.* [47]. They agree well with our calculations.

(b) One question of interest concerns the role of negative spectrum ($n < 0$) of the Dirac-Coulomb Sturmians of first order in relativistic two-photon calculations. We see the effects arising from the summation over the non-negative ($n \geq 0$) and negative parts of the spectrum. In Fig. 3, $W_+^{(R)}$ contributions in the available domain experience, at the most, a 8.5% divergence with increasing Z . Instead, in Fig. 4, the inverse tendency is observed with the multipole $E1M1$ for which, at low Z , the relative error is about 68% and decreases with the growth of the nuclear charge. As for $W_-^{(R)}$, it lies, in general, between 80% and 100% and is almost constant, regardless of the multipole considered, except $M1M2$ for which it decreases when Z increases. A perusal of the different

TABLE V. Contributions from different combinations of multipoles to the integrated two-photon decay rates $W(s^{-1})$ for the transition $2p_{1/2} \rightarrow 1s_{1/2}$ as a function of the nuclear charge. First entry: $W^{(R)}$; second entry: $W^{(A)}$ (Amaro *et al.* [47]); third entry: $W^{(L)}$ (Labzowsky *et al.* [45]); fourth entry: $W^{(So)}$ (Solov'yev *et al.* [36], Labzowsky *et al.* [35]). Powers of ten are given in parentheses.

Z	$W(E1M1)$	$W(E1E2)$	$W(M1M2)$
1	9.676656(−6)	6.611798(−6)	3.827879(−17)
	9.676654(−6)	6.61179(−6)	3.827877(−17)
	9.667(−6)	6.605(−6)	
	9.677(−6)	6.673(−6)	
	40	6.027546(7)	4.092510(7)
		6.027323(7)	4.092020(7)
		6.020(7)	4.088(7)
		6.341(7)	4.374(7)
	92	3.876927(10)	2.374811(10)
		3.863302(10)	2.358404(10)
80		3.859(10)	2.357(10)
		4.966(10)	3.425(10)

TABLE VI. Contributions from different combinations of multipoles to the integrated two-photon decay rates $W(s^{-1})$ for the transition $2s_{1/2} \rightarrow 1s_{1/2}$ as a function of the nuclear charge. First entry: $W^{(R)}$; second entry: $W_+^{(R)}$; third entry: $W_-^{(R)}$; fourth entry: $W^{(L)}$ (Labzowsky *et al.* [45]); fifth entry: $W^{(NR)}$ [Eqs. (74)–(78)]; sixth entry: $W^{(PJ)}$ (Parpia and Johnson [43]); seventh entry: $W^{(GD)}$ (Goldman and Drake [41]). Powers of ten are given in parentheses.

Z	$W(2E1)$	$W(E1M2)$	$W(2M1)$	$W(2E2)$	$W(2M2)$	$W(E2M1)$
1	8.229061	2.537181(-10)	1.380358(-11)	4.907230(-12)	3.069352(-22)	1.639357(-23)
	8.229040	2.055791(-10)	2.862986(-11)	4.907198(-12)	2.122096(-22)	1.701738(-13)
	1.530988(-11)	3.241807(-12)	2.867209(-12)	5.184052(-23)	1.538559(-23)	1.701705(-13)
	8.2207			4.907313(-12)		
	8.229352					
	8.2291					
	8.2291	2.5371(-10)	1.3804(-11)	4.9072(-12)	4.089(-22)	1.638(-23)
10	8.200647(6)	2.528056(0)	1.386428(-1)	4.898993(-2)	3.068670(-8)	1.661757(-9)
	8.198545(6)	2.046950(0)	2.870806(-1)	4.895813(-2)	2.119324(-8)	1.700698(-3)
	1.539192(-1)	3.241873(-2)	2.872111(-2)	5.198844(-9)	1.542755(-9)	1.697410(-3)
	8.1922(6)			4.907313(-2)		
	8.229352(6)					
20	5.195137(8)	2.562369(3)	1.439270(2)	4.990921(1)	5.024838(-4)	2.837239(-5)
	5.189731(8)	2.070584(3)	2.964618(2)	4.977879(1)	3.458898(-4)	1.738546(0)
	1.601902(2)	3.319877(1)	2.956499(1)	8.591912(-5)	2.548792(-5)	1.724818(0)
	5.1899(8)			5.025089(1)		
	5.266785(8)					
	5.1965(8)					
	5.1956(8)	2.5629(3)	1.4383(2)	4.9909(1)	6.714(-4)	2.838(-5)
30	5.821131(9)	1.454723(5)	8.502323(3)	2.853190(3)	1.465996(-1)	8.875376(-3)
	5.807171(9)	1.171943(5)	1.734783(4)	2.836231(3)	1.003567(-1)	1.000196(2)
	9.491238(3)	1.914590(3)	1.720215(3)	2.544985(-2)	7.546683(-3)	9.818067(1)
	5.8152(9)			2.897719(3)		
	5.999198(9)					
40	3.198673(10)	2.532719(6)	1.566111(5)	5.004195(4)	8.226284(0)	5.491783(-1)
	3.184582(10)	2.032494(6)	3.148449(5)	4.950494(4)	5.587471(0)	1.772345(3)
	1.750945(5)	3.400288(4)	3.094818(4)	1.458049(0)	4.322669(-1)	1.711625(3)
	3.1953(10)			5.145691(4)		
	3.370743(10)					
	3.1996(10)					
	3.1988(10)	2.5329(6)	1.5496(5)	5.0042(4)	1.109(1)	5.492(-1)
50	1.186662(11)	2.305484(7)	1.536359(6)	4.584559(5)	1.872267(2)	1.417839(1)
	1.178150(11)	1.841803(7)	3.022465(6)	4.506120(5)	1.258711(2)	1.649652(4)
	1.713218(6)	3.167169(5)	2.933682(5)	3.405592(1)	1.010030(1)	1.555979(4)
	1.1854(11)			4.792298(5)		
	1.285836(11)					
60	3.426718(11)	1.392205(8)	1.021430(7)	2.779868(6)	2.411130(3)	2.131864(2)
	3.389519(11)	1.106667(8)	1.949330(7)	2.709622(6)	1.600265(3)	1.024470(5)
	1.127393(7)	1.961221(6)	1.858948(6)	4.521682(2)	1.343099(2)	9.346472(4)
	3.4230(11)			2.967265(6)		
	3.839486(11)					
	3.4270(11)					
	3.4267(11)	1.3922(8)	9.6776(6)	2.7799(6)	3.304(3)	2.132(2)
70	8.307144(11)	6.334205(8)	5.248247(7)	1.265224(7)	2.099927(4)	2.233543(3)
	8.177038(11)	5.008344(8)	9.611343(7)	1.220338(7)	1.371925(4)	4.832255(5)
	5.664943(7)	9.162123(6)	8.946377(6)	4.075960(3)	1.214996(3)	4.208112(5)
	8.2975(11)			1.386194(7)		
	9.681750(11)					
80	1.767607(12)	2.343214(9)	2.261100(8)	4.656789(7)	1.377013(5)	1.818633(4)
	1.728932(12)	1.842535(9)	3.921825(8)	4.432792(7)	8.826223(4)	1.875808(6)

TABLE VI. (*Continued.*)

Z	$W(2E1)$	$W(E1M2)$	$W(2M1)$	$W(2E2)$	$W(2M2)$	$W(E2M1)$
90	2.345555(8)	3.481952(7)	3.532552(7)	2.774577(4)	8.327096(3)	1.530759(6)
	1.7655(12)					
	2.157275(12)			5.269187(7)		
	1.7675(12)					
	1.7679(12)	2.3431(9)	1.9045(8)	4.6568(7)	1.932(5)	1.819(4)
	3.393951(12)	7.403744(9)	8.641852(8)	1.452950(8)	7.295258(5)	1.238932(5)
	3.292413(12)	5.789315(9)	1.398025(9)	1.360439(8)	4.569426(5)	6.338603(6)
	8.409672(8)	1.129956(8)	1.204652(8)	1.528426(5)	4.642472(4)	4.721585(6)
	3.3899(12)					
	4.373415(12)			1.711074(8)		
100	5.981423(12)	2.066445(10)	3.061347(9)	3.962382(8)	3.283020(6)	7.468695(5)
	5.739900(12)	1.606952(10)	4.539131(9)	3.633584(8)	1.999435(6)	1.951263(7)
	2.702869(9)	3.235652(8)	3.682911(8)	7.148751(5)	2.216097(5)	1.276734(7)
	5.9783(12)					
	8.229352(12)			4.907313(8)		

curves in Figs. 5 and 6 reveals that the contribution of the negative part of the Sturmian basis to the spectral distribution is also negligible for the leading multipole $2E1$ as well as $2E2$ and $E1E2$ channels, but becomes rather pronounced for the higher ones, $M1M2$ and $E2M1$. From what precedes, it is apparent that the exclusion of the negative spectrum from the intermediate-state summation leads to either a reduction or an increase of the fully relativistic decay rate. Likewise, interferences between the non-negative and negative parts of the complete set of relativistic Sturmian functions of the first order manifest themselves, particularly in the case of the $E2M1$ channel for which $W_+^{(R)}$ and $W_-^{(R)}$ are each about ten orders of magnitude higher than $W^{(R)}$ if decay of medium- and high- Z ions is considered. Their combination obviously yields the cancellation observed.

As pointed out in Sec. II, it is important to examine the influence of retardation terms in Eq. (42) and compare with preserving the full spherical Bessel functions in the radial integrals. Switching our attention to Figs. 7 and 8, which show the same tendencies, we can check the numerical accuracy of this truncation scheme in the calculation of radial integrals and, therefore, of the emission probabilities. Retaining only the first retardation term in the series expansion of the spherical Bessel functions leads, beyond $Z = 25$, to a big deviation from the fully relativistic spectral distribution. Therefore, the range of validity of this term is narrower. In contrast, considering the leading two terms, one finds almost identical results with a relative error of less than 10^{-7} for all multipole decay channels. This agreement explains why numbers of the latter case are not given in the tables. It then becomes evident in

TABLE VII. Contributions from different combinations of multipoles to the integrated two-photon decay rates $W(s^{-1})$ for the transition $2s_{1/2} \rightarrow 1s_{1/2}$ as a function of the nuclear charge. First entry: $W^{(R)}$; second entry: $W^{(\tilde{S}a)}$ (Santos *et al.* [44]); third entry: $W^{(GD)}$ (Goldman and Drake [41]); fourth entry: $W^{(PJ)}$ (Parpia and Johnson [43]); fifth entry: $W^{(A)}$ (Amaro *et al.* [55]); sixth entry: $W^{(L)}$ (Labzowsky *et al.* [45]); seventh entry: $W^{(G)}$ (Goldman [87]). Powers of ten are given in parentheses.

Z	$W(2E1)$	$W(E1M2)$	$W(2M1)$	$W(2E2)$	$W(2M2)$	$W(E2M1)$
1	8.229061	2.537181(-10)	1.380358(-11)	4.907230(-12)	3.069352(-22)	1.639357(-23)
	8.229063	2.537183(-10)	1.380359(-11)	4.907232(-12)	3.069354(-22)	1.637802(-23)
	8.2291	2.5371(-10)	1.3804(-11)	4.9072(-12)	4.089(-22)	1.638(-23)
	8.2291					
	8.2290591586	2.5371807735(-10)	1.3803580496(-11)	4.9072289232(-12)	3.0693510074(-22)	1.6393565197(-23)
	8.2207					
	8.22906	2.53718(-10)	1.38036(-11)	4.90723(-12)	3.06935(-22)	1.63936(-23)
	54	1.859308(11)	4.928837(7)	3.403959(6)	9.820835(5)	5.504194(2)
		1.859221(11)	4.927784(7)	3.402664(6)	9.817756(5)	5.502043(2)
92	3.825895(12)	9.173468(9)	1.118273(9)	1.793657(8)	9.971596(5)	1.789081(5)
	3.825552(12)	9.138566(9)	1.109270(9)	1.785817(8)	9.906518(5)	1.766901(5)
	3.8259(12)	9.1734(9)	8.2664(8)	1.7936(8)	1.425(6)	1.790(5)
	3.8257(12)					
	3.825839(12)					
	3.8216(12)					

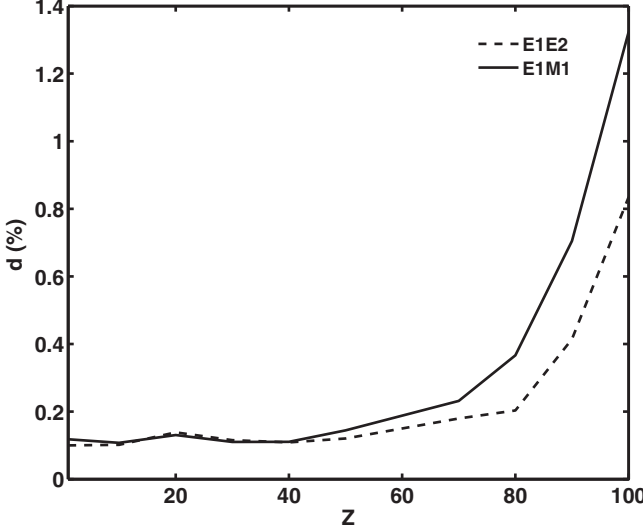


FIG. 1. An illustration of the behavior of the percentage difference d between W^R (this work) and W^L (Ref. [45]) total two-photon decay rates for the transitions $2p_{1/2} \rightarrow 1s_{1/2}$ ($E1M1$; $E1E2$) vs the nuclear charge Z . Curves are drawn to guide the eye.

this semirelativistic approach that Eq. (41), with the first two terms in Gauss hypergeometric functions, is a simple formula leading to a fast procedure for the computation of two-photon decay rates.

We now focus our attention on Fig. 9, where the normalized integrated decay rate for the $E1E2$, $2E1$, and $2E2$ multipoles are plotted as a function of the nuclear charge. The horizontal dotted line represents the nonrelativistic result as described in Sec. III. As expected and previously pointed out in Ref. [88], corrections arising from relativity are evident, namely, that the magnitude of $\phi(Z)$ is significantly lowered with the growth of

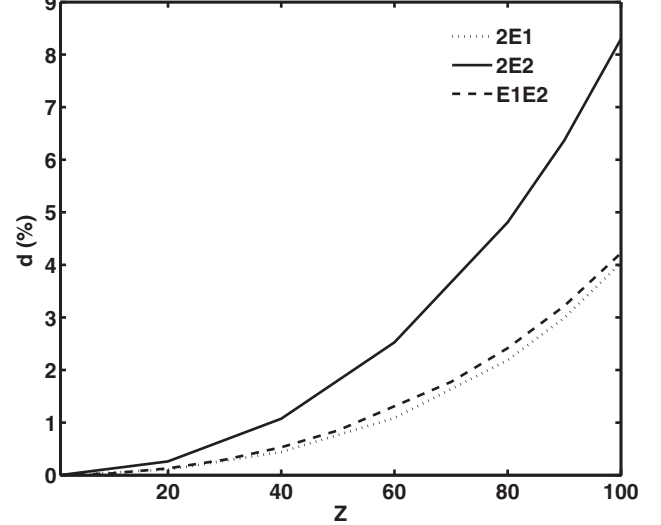


FIG. 3. An illustration of the behavior of the percentage difference d between W^R (this work) and W_+^R total two-photon decay rates for the transitions $2p_{1/2} \rightarrow 1s_{1/2}$ ($E1E2$) and $2s \rightarrow 1s$ ($2E1$; $2E2$) vs the nuclear charge Z . Curves are drawn to guide the eye.

Z . Also the influence of the negative part of the Dirac-Coulomb Sturmian basis set is apparent when considering higher Z .

Finally, in Table VIII are compiled full relativistic multipole values of emission probabilities for the transition $2s_{1/2} \rightarrow 1s_{1/2}$ computed from our formulation, as well as the contributions calculated by Santos *et al.* [44] and Goldman and Drake [41]. Enough multipoles have been included in the computations. Percentage differences defined previously are plotted in Fig. 10. As one can see from this figure, they are within 0.06%. However, results from Ref. [41] are closer to those of this work for $Z \geq 40$.

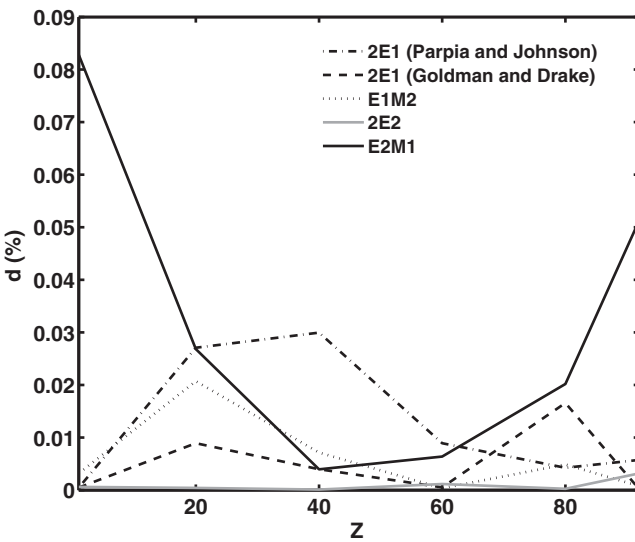


FIG. 2. An illustration of the behavior of the percentage difference d between W^R (this work), W^{GD} (Ref. [41]), and $W^{(P)}$ (Ref. [43]) total two-photon decay rates for the transitions $2s_{1/2} \rightarrow 1s_{1/2}$ ($2E1$; $E1M2$; $2E2$; $E2M1$) vs the nuclear charge Z . Curves are drawn to guide the eye.

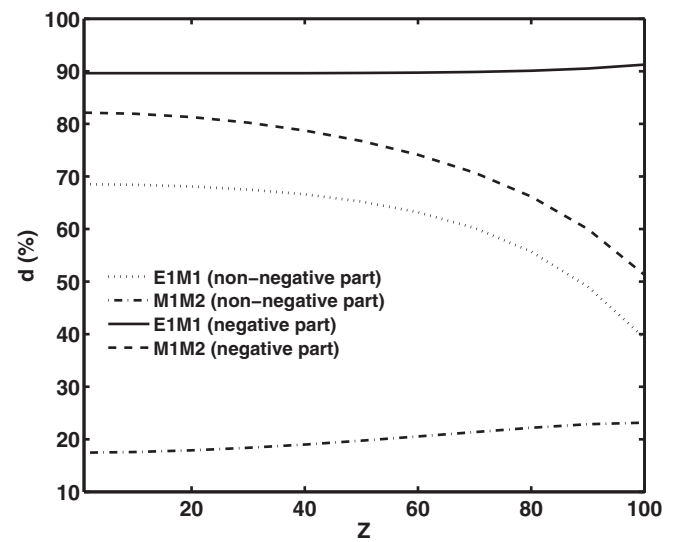


FIG. 4. An illustration of the behavior of the percentage difference d between W^R and W_+^R ($E1M1$: dotted line; $M1M2$: dashed dotted line), W^R ($E1M1$: solid dark line; $M1M2$: dashed line) total two-photon decay rates for the transitions $2p_{1/2} \rightarrow 1s_{1/2}$ vs the nuclear charge Z . Curves are drawn to guide the eye.

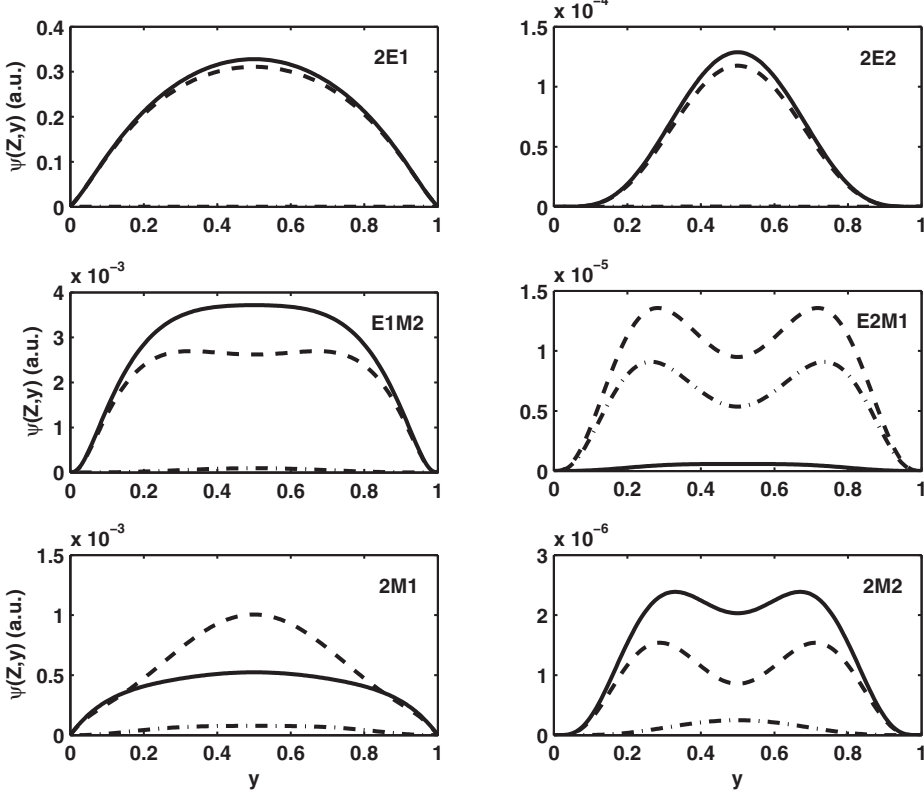


FIG. 5. Shape of the spectral distribution function $\psi(Z,y)$ of the $2E1$, $2E2$, $E1M2$, $E2M1$, $2M1$, and $2M2$ contributions for the transition $2s_{1/2} \rightarrow 1s_{1/2}$ at the nuclear charge $Z = 100$. The variable y is the fraction of energy carried by one of the two photons. The solid dark line, dashed line, and dash-dotted line represent the results using Sturmian basis sets with the radial quantum number $-n_{\max} \leq n \leq n_{\max}$, $0 \leq n \leq n_{\max}$, and $-n_{\max} \leq n \leq -1$, respectively.

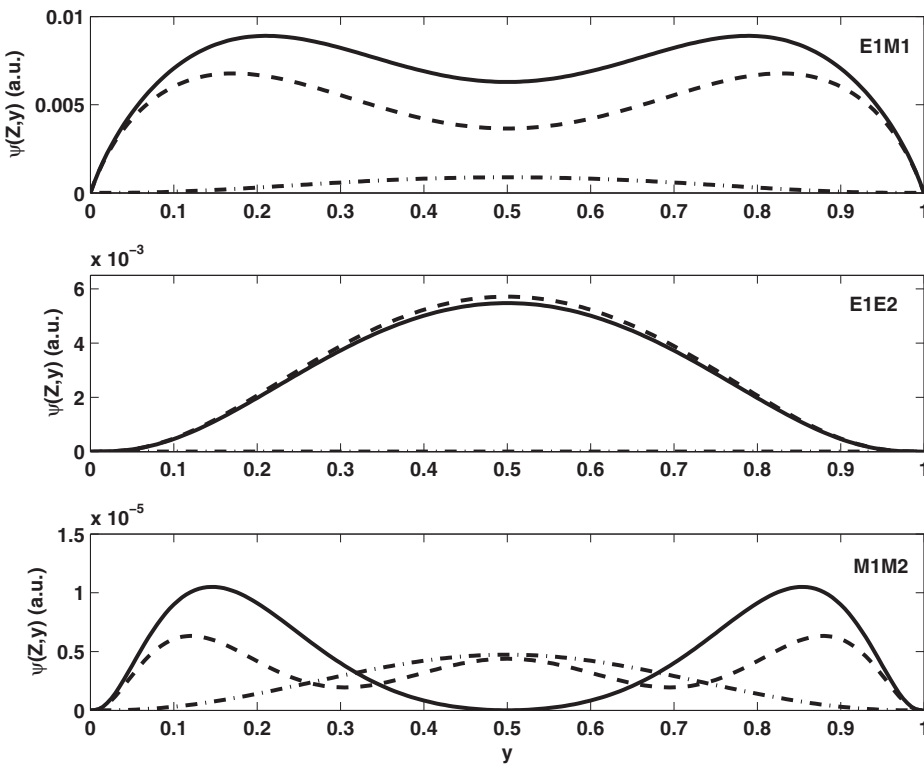


FIG. 6. Shape of the spectral distribution function $\psi(Z,y)$ of the $E1M1$, $E1E2$, and $M1M2$ contributions for the transition $2p_{1/2} \rightarrow 1s_{1/2}$ at the nuclear charge $Z = 100$. The variable y is the fraction of energy carried by one of the two photons. The dashed, solid-dark, and dash-dotted lines represent the results using Sturmian basis sets, respectively, with the radial quantum number $-n_{\max} \leq n \leq n_{\max}$, $0 \leq n \leq n_{\max}$, and $-n_{\max} \leq n \leq -1$, respectively.

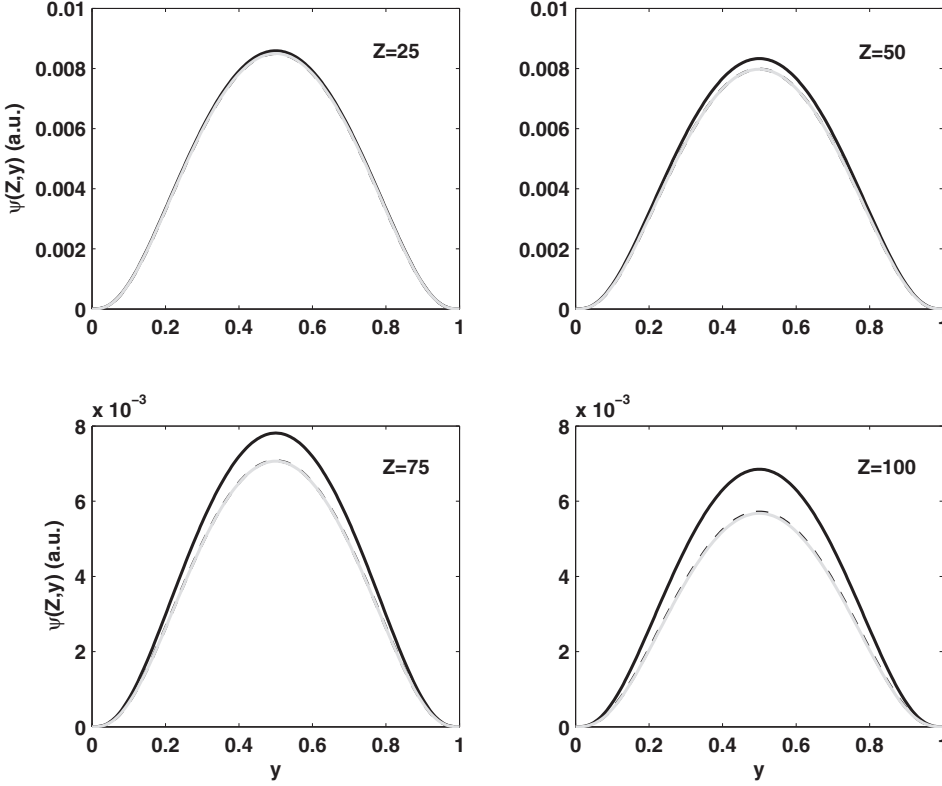


FIG. 7. Plot of the spectral distribution function $\psi(Z,y)$ of the $E1E2$ contribution for the transition $2p_{1/2} \rightarrow 1s_{1/2}$ at the nuclear charges $Z = 25, 50, 75$, and 100 . The variable y is the fraction of energy carried by one of the two photons. The solid dark and solid light gray lines represent computations by retaining only the first and the leading two retardation terms, respectively, in the series expansion of the spherical Bessel functions in the transition operator. The dashed line represents the fully relativistic multipole calculations.

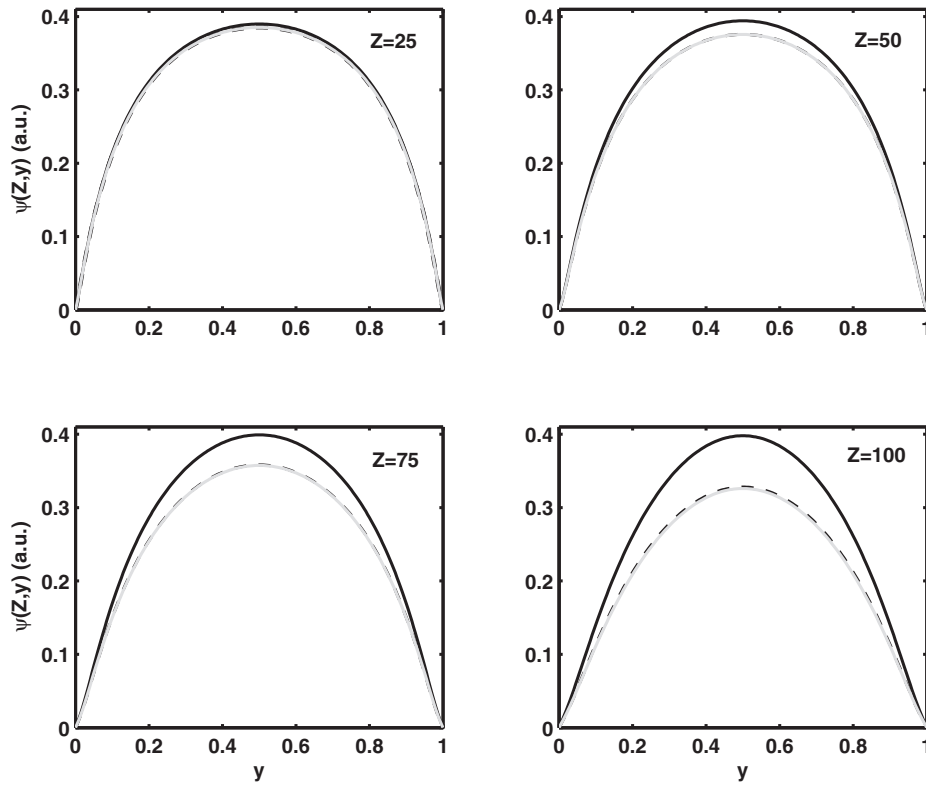


FIG. 8. Plot of the spectral distribution function $\psi(Z,y)$ of the $2E1$ contribution for the transition $2s_{1/2} \rightarrow 1s_{1/2}$ at the nuclear charges $Z = 25, 50, 75$, and 100 . The variable y is the fraction of energy carried by one of the two photons. The solid dark and solid light gray lines represent computations by retaining only the first and the leading two retardation terms, respectively, in the series expansion of the spherical Bessel functions in the transition operator. The dashed line represents the fully relativistic multipole calculations.

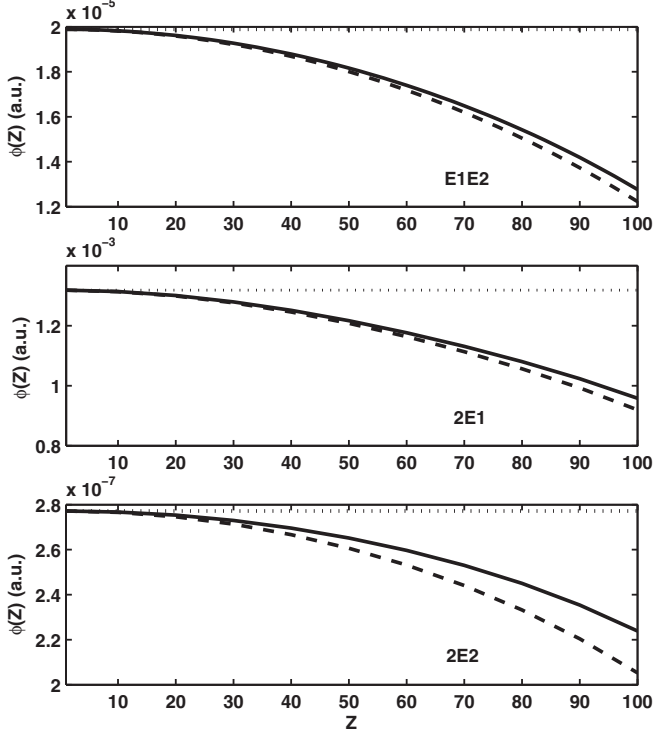


FIG. 9. Plot of the normalized integrated decay rate $\phi(Z)$ for the transitions $2p_{1/2} \rightarrow 1s_{1/2}$ ($E1E2$) and $2s_{1/2} \rightarrow 1s_{1/2}$ ($2E1$; $2E2$) vs the nuclear charge Z . The dotted line represents the nonrelativistic results; the solid dark and dashed lines represent the computations using Sturmian basis sets with the radial quantum number $-n_{\max} \leq n \leq n_{\max}$ and $0 \leq n \leq n_{\max}$, respectively.

V. CONCLUDING REMARKS

In this paper, we have undertaken, through a systematic study, a comparison of our DCGF approach with other refined computations of two-photon transitions $2p_{1/2} \rightarrow 1s_{1/2}$ and $2s_{1/2} \rightarrow 1s_{1/2}$ in the hydrogen atom and hydrogenlike ions with an infinitely heavy, pointlike, and spinless nucleus of

TABLE VIII. Total two-photon decay rates $W(s^{-1})$ of the $2s_{1/2}$ state as a function of the nuclear charge. $W^{(R)}$; $W^{(S)}$ (Santos *et al.* [44]); $W^{(GD)}$ (Goldman and Drake [41]). Powers of ten are given in parentheses.

Z	$W^{(R)}$	$W^{(S)}$	$W^{(GD)}$
1	8.229061	8.229063	8.2291
10	8.200650(6)	8.200570(6)	8.2010(6)
20	5.195165(8)	5.194978(8)	5.1956(8)
30	5.821288(9)	5.821062(9)	5.8217(9)
40	3.198947(10)	3.198853(10)	3.1990(10)
50	1.186912(11)	1.186870(11)	1.1869(11)
60	3.428240(11)	3.428003(11)	3.4282(11)
70	8.314130(11)	8.313011(11)	8.3139(11)
80	1.770223(12)	1.769879(12)	1.7701(12)
90	3.402365(12)	3.401841(12)	3.4021(12)
92	3.836367(12)	3.835980(12)	3.8361(12)
100	6.005549(12)	6.008640(12)	6.0045(12)

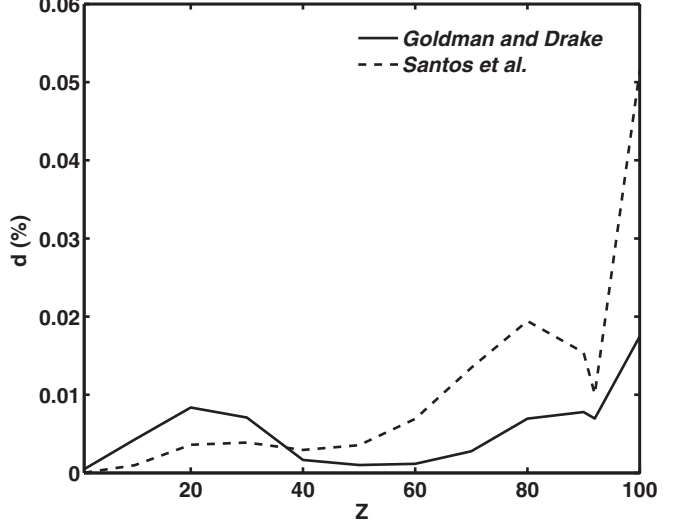


FIG. 10. An illustration of the behavior of the percentage difference d between our W^R and the W^{GD} (Ref. [41]) and W^S (Ref. [44]) total two-photon decay rates for the transitions $2s_{1/2} \rightarrow 1s_{1/2}$ ($2E1$; $E1E2$; $2E2$; $E2M1$) vs the nuclear charge Z . Curves are drawn to guide the eye.

charge ranging from 1 to 100. To this end, we have derived analytical relativistic formulas for spectral distributions and total decay rates by using the Sturmian expansion of the complete first-order Dirac-Coulomb Green function constructed by Szmytkowski. These formulas are quite general and may be applied to any multipole of the two photons. We have then checked that for three particular multipole cases, namely, $E1E2$, $2E1$, and $2E2$, they recover those of the nonrelativistic formulation based on the well-known Schrödinger-Coulomb Green function expanded over the Coulomb Sturmian basis. In addition, by making use of two appropriate methods, radial integrals involved in matrix elements have been treated with great care, and we have obtained extremely accurate values. With these formulas, convenient for computer calculations, we have carried out numerical evaluations of the most significant multipole contributions to the above-mentioned transitions. In accordance with Grant's demonstration, our fully relativistic multipole results show a perfect agreement between gauges. On the other hand, the influence of retardation as well as the effects of the negative spectrum of the Sturmian basis have been estimated. Concerning the first point, the leading two retardation terms in the series expansion of spherical Bessel functions in the transition operator yield very accurate results. This approximate procedure enables one also to save some computation time. As for the second point, we have observed in some multipole channels, e.g., $E2M1$ and $M1M2$, important interferences between the non-negative and negative parts of the complete set of relativistic Sturmian functions. However, these effects arise not only for rather heavy ions. Finally, the percentage differences between our predictions and theoretical data from Goldman and Drake, Santos *et al.*, Amaro *et al.*, and Parpia and Johnson are within 0.08%, except for multipoles with only magnetic components such as $2M1$ and $2M2$. The results of these authors are closer to ours than those of Labzowsky *et al.* for which the d numbers lie between

0.1% and 1.4%. In light of what precedes, we strongly believe that the present DCGF scheme provides a reliable, efficient, and valuable tool regarding the study of two-photon and even higher-order atomic processes.

ACKNOWLEDGMENTS

The authors are grateful to the Abdus Salam International Centre for Theoretical Physics (ICTP) for its support through the OEA-AC-71 project. The Centre for Atomic Molecular Physics and Quantum Optics (CEPAMOQ) of the University of Douala (Cameroon) is the ICTP Affiliated Centre in Central Africa. The authors express their gratitude to Prof. B. Piraux, Prof. Yu. V. Popov, and Prof. G. Gasaneo for fruitful discussions about many aspects of Sturmian functions and their numerical implementation. We are grateful to the referee

for his valuable criticisms and fruitful suggestions which have been used to improve an earlier version of this manuscript.

APPENDIX A: COULOMB STURMIAN REPRESENTATION OF GREEN AND HYDROGENIC BOUND-STATE FUNCTIONS

In order to make our text self-contained, we briefly recall below relativistic and nonrelativistic representations of Green and hydrogenic bound-state functions expressed in terms of the Coulomb Sturmian functions.

1. Relativistic representation

The relativistic atomic units (r.a.u.) are used here. In a remarkable work, Szmytkowski [72] constructed the four-component Dirac-Coulomb Sturmian basis $\{\Phi_{nkm}(\mathbf{r}, E)\}$ of the first order,

$$\Phi_{nkm}(\mathbf{r}, E) = \frac{1}{r} \begin{pmatrix} S_{nk}(x) \Omega_{km}(\hat{\mathbf{r}}) \\ i T_{nk}(x) \Omega_{-km}(\hat{\mathbf{r}}) \end{pmatrix}, \quad (\text{A1})$$

and derived the following Sturmian expansions of the Dirac-Coulomb Green function:

$$G_E(\mathbf{r}, \mathbf{r}') = \sum_{km} \frac{1}{rr'} \begin{pmatrix} g_k^{(11)} \Omega_{km}(\hat{\mathbf{r}}) \Omega_{km}^\dagger(\hat{\mathbf{r}'}) & -ig_k^{(12)} \Omega_{km}(\hat{\mathbf{r}}) \Omega_{-km}^\dagger(\hat{\mathbf{r}'}) \\ ig_k^{(21)} \Omega_{-km}(\hat{\mathbf{r}}) \Omega_{km}^\dagger(\hat{\mathbf{r}'}) & g_k^{(22)} \Omega_{-km}(\hat{\mathbf{r}}) \Omega_{-km}^\dagger(\hat{\mathbf{r}'}) \end{pmatrix}, \quad (\text{A2})$$

with

$$\begin{aligned} g_k^{(11)}(E; r, r') &= \sum_{n=-\infty}^{\infty} \tilde{\theta}_{nk} S_{nk}(x) S_{nk}(x'), \\ g_k^{(12)}(E; r, r') &= \sum_{n=-\infty}^{\infty} \tilde{\alpha}_{nk} S_{nk}(x) T_{nk}(x'), \\ g_k^{(21)}(E; r, r') &= \sum_{n=-\infty}^{\infty} \tilde{\theta}_{nk} T_{nk}(x) S_{nk}(x'), \\ g_k^{(22)}(E; r, r') &= \sum_{n=-\infty}^{\infty} \tilde{\alpha}_{nk} T_{nk}(x) T_{nk}(x'). \end{aligned} \quad (\text{A3})$$

The radial Sturmians may be written in terms of the generalized Laguerre polynomials [86] of the same order 2γ , as

$$S_{nk}(x) = x^\gamma e^{-x/2} [A_{nk} L_{|n|-1}^{(2\gamma)}(x) + B_{nk} L_{|n|}^{(2\gamma)}(x)], \quad (\text{A5})$$

$$T_{nk}(x) = \varepsilon x^\gamma e^{-x/2} [A_{nk} L_{|n|-1}^{(2\gamma)}(x) - B_{nk} L_{|n|}^{(2\gamma)}(x)]. \quad (\text{A6})$$

They are normalized according to the following orthonormality relations:

$$\frac{1}{2} \int_0^\infty dx [\varepsilon S_{nk}(x) S_{n'k}(x) + \varepsilon^{-1} T_{nk}(x) T_{n'k}(x)] = \delta_{nn'},$$

$$\int_0^\infty dx \frac{\mathcal{Z}}{x} [\mu_{nk} S_{nk}(x) S_{n'k}(x) - \mu_{nk}^{-1} T_{nk}(x) T_{n'k}(x)] = \delta_{nn'}.$$

Notice that we define $L_{-1}^{(\beta)}(x) = 0$. For convenience, the arguments are chosen to be $x = 2\lambda r$, $x' = 2\lambda r'$. E and Z

are fixed real parameters such that $0 < \mathcal{Z} < 1$, $0 < E < 1$.

$$\mathcal{Z} = \alpha Z, \quad \gamma = \sqrt{\kappa^2 - \mathcal{Z}^2}, \quad \lambda = \sqrt{1 - E^2}, \quad \varepsilon = \sqrt{\frac{1 - E}{1 + E}}, \quad (\text{A7})$$

where α is the Sommerfeld fine-structure constant, and

$$\begin{aligned} \tilde{\theta}_{nk} &= \frac{\mu_{nk}}{\mu_{nk} - 1}, \quad \tilde{\alpha}_{nk} = \tilde{\theta}_{nk} - 1, \\ \mu_{nk} &= \varepsilon \mathcal{Z}^{-1} (|n| + \gamma \pm N_{nk}), \end{aligned} \quad (\text{A8})$$

$$\begin{aligned} A_{nk} &= \sqrt{\frac{(|n| + 2\gamma) |n|!}{2\varepsilon N_{nk} (N_{nk} \mp \kappa) \Gamma(|n| + 2\gamma)}}, \\ B_{nk} &= \frac{\kappa \mp N_{nk}}{|n| + 2\gamma} A_{nk}, \quad N_{nk} = \sqrt{(|n| + \gamma)^2 + \mathcal{Z}^2}. \end{aligned} \quad (\text{A9})$$

The angular quantum number κ takes all integer values except zero according to $\kappa = \epsilon(j + 1/2)$, $j = l - \epsilon/2 = \bar{l} + \epsilon/2$, $\epsilon = \pm 1$. l and j are the electron orbital and total angular momenta. The following sign convention is adopted in relations (A8) and (A9). The upper sign should be chosen for $n > 0$, while the lower one should be chosen for $n < 0$. For $n = 0$, one must choose the upper sign if $\kappa < 0$ and the lower one if $\kappa > 0$.

For hydrogenic ions of nuclear charge Z , bispinor bound states used in this work read

$$\Psi_{nkm}(\mathbf{r}) = \frac{1}{r} \begin{pmatrix} P_{nk}(r) \Omega_{km}(\hat{\mathbf{r}}) \\ i Q_{nk}(r) \Omega_{-km}(\hat{\mathbf{r}}) \end{pmatrix}, \quad (\text{A10})$$

$$P_{nk}(r) = x^\gamma e^{-x/2} [C_{nk} L_{|n|-1}^{(2\gamma)}(x) + D_{nk} L_n^{(2\gamma)}(x)], \quad (\text{A11})$$

$$Q_{nk}(r) = x^\gamma e^{-x/2} [\tilde{C}_{nk} L_{n-1}^{(2\gamma)}(x) - \tilde{D}_{nk} L_n^{(2\gamma)}(x)], \quad (\text{A12})$$

where

$$C_{nk} = \sqrt{\frac{\lambda_{nk} (1 + E_{nk})(n + 2\gamma)n!}{2N_{nk}(N_{nk} - \kappa)\Gamma(n + 2\gamma)}}, \quad (\text{A13})$$

$$\tilde{C}_{nk} = \sqrt{\frac{\lambda_{nk} (1 - E_{nk})(n + 2\gamma)n!}{2N_{nk}(N_{nk} - \kappa)\Gamma(n + 2\gamma)}},$$

$$D_{nk} = \frac{\kappa - N_{nk}}{n + 2\gamma} C_{nk}, \quad \tilde{D}_{nk} = \frac{\kappa - N_{nk}}{n + 2\gamma} \tilde{C}_{nk}, \quad (\text{A14})$$

$$\lambda_{nk} \equiv \lambda(E_{nk}) = \frac{Z}{N_{nk}},$$

$$E_{nk} = (n + \gamma)/N_{nk}, \quad n = 0, 1, 2, \dots \quad (\text{A15})$$

The above radial functions are related to the radial Sturmians by $P_{nk}(r) = \lambda_{nk} S_{nk}(2\lambda_{nk}r)$ and $Q_{nk}(r) = \lambda_{nk} T_{nk}(2\lambda_{nk}r)$. They are normalized according to the condition

$$\int_0^\infty dr [P_{nk}^2(r) + Q_{nk}^2(r)] = 1.$$

It should also be noted that the radial quantum number n is relied to the principal quantum number \tilde{n} by $n = \tilde{n} - |\kappa|$.

2. Nonrelativistic representation

The atomic units (a.u.) are used throughout this section. In this case, the Green function is represented by an infinite sum over the discrete Sturmian basis functions of the Schrödinger equation [62,89,90],

$$G_\xi(\mathbf{r}, \mathbf{r}') = \sum_{l,m} \frac{1}{rr'} g_l(\xi; r, r') Y_{lm}(\hat{\mathbf{r}}) Y_{lm}^*(\hat{\mathbf{r}}'), \quad (\text{A16})$$

$$g_l(\xi; r, r') = \frac{1}{\lambda} \sum_{n=0}^{\infty} \frac{n+l+1}{\lambda(n+l+1) - Z} S_{nl}(r) S_{nl}(r'),$$

$$S_{nl}(r) = \sqrt{\frac{\lambda n!}{(n+l+1)(n+2l+1)!}} x^{l+1} e^{-x/2} L_n^{(2l+1)}(x), \quad (\text{A17})$$

$$\lambda = \sqrt{-2\xi}, \quad x = 2\lambda r, \quad x' = 2\lambda r'.$$

These radial Sturmian functions $S_{nl}(r)$ are normalized in such a way that [91]

$$\int_0^\infty dr S_{n'l}(r) S_{nl}(r) = \begin{cases} 1, & n' = n \\ -\frac{1}{2}\sqrt{\frac{n(n+2l+1)}{(n+l)(n+l+1)}}, & n' = n-1 \\ -\frac{1}{2}\sqrt{\frac{(n+1)(n+2l+2)}{(n+l+1)(n+l+2)}}, & n' = n+1 \\ 0, & \text{otherwise,} \end{cases}$$

and

$$\int_0^\infty dr S_{nl}(r) \frac{1}{r} S_{n'l}(r) = \frac{\lambda}{n+l+1} \delta_{nn'}.$$

It should be noted that they are exact solutions of the Schrödinger equation for bound states of hydrogenic ions [82]

when $\lambda \equiv \lambda_n = Z/(n+l+1)$, that is,

$$\psi_{nlm}(\mathbf{r}) = \frac{1}{r} P_{nl}(r) Y_{lm}(\hat{\mathbf{r}}), \quad P_{nl}(r) = S_{nl}(2\lambda_n r), \quad (\text{A18})$$

$$\lambda_n = \sqrt{-2\xi_n}, \quad \xi_n = -\frac{Z^2}{2(n+l+1)^2}, \quad n = 0, 1, 2, \dots \quad (\text{A19})$$

APPENDIX B: REDUCTION TO RADIAL INTEGRALS OF MATRIX ELEMENTS

Let us introduce the following notations: $\mathbf{T}_{LM}^{(1)} = A_{LM}^{(1)*}$, $\mathbf{T}_{LM}^{(0)} = A_{LM}^{(0)*}$, $\mathbf{T}_{LM} = \Phi_{LM}^*$ for emission, and $\mathbf{T}_{LM}^{(1)} = A_{LM}^{(1)}$, $\mathbf{T}_{LM}^{(0)} = A_{LM}^{(0)}$, $\mathbf{T}_{LM} = \Phi_{LM}$ for absorption. These multipole field irreducible tensor operators of order L are given by Eqs. (8)–(11). Following the works of Grant [85] and Armstrong *et al.* [92] and making use of the Wigner-Eckart theorem, we get, in the general form,

$$\langle \sigma | \boldsymbol{\alpha} \cdot \mathbf{T}_{LM}^{(1)} | \tau \rangle = i^L \sqrt{4\pi} a b (\mathcal{F}_{\sigma\tau} - G_L \mathcal{H}_{\sigma\tau}), \quad (\text{B1})$$

$$\langle \sigma | \boldsymbol{\alpha} \cdot \mathbf{T}_{LM}^{(0)} | \tau \rangle = i^{L+1} a b \mathcal{T}_{\sigma\tau}, \quad (\text{B2})$$

$$\langle \sigma | \mathbf{T}_{LM} | \tau \rangle = \pm i^L a b \mathcal{L}_{\sigma\tau}. \quad (\text{B3})$$

In Eq. (B3), the upper and lower signs refer to emission and absorption, respectively. On the other hand,

$$b = [j_\sigma, j_\tau]^{1/2} \begin{pmatrix} j_\sigma & L & j_\tau \\ 1/2 & 0 & -1/2 \end{pmatrix} \Pi(j_\sigma, j_\tau, L), \quad (\text{B4})$$

$$a = \begin{cases} (-1)^{j_\sigma + j_\tau + m_\tau + 1/2} \begin{pmatrix} j_\sigma & L & j_\tau \\ m_\sigma & M & -m_\tau \end{pmatrix} & \text{for emission,} \\ (-1)^{m_\sigma - 1/2} \begin{pmatrix} j_\sigma & L & j_\tau \\ -m_\sigma & M & m_\tau \end{pmatrix} & \text{for absorption.} \end{cases} \quad (\text{B5})$$

The parity selection rules follow from the calculation of the reduced matrix elements. For electric multipoles, $\Pi(j_\sigma, j_\tau, L) = 1$ for $\kappa_\sigma \kappa_\tau > 0$, $j_\sigma + j_\tau + L$ odd or $\kappa_\sigma \kappa_\tau < 0$, $j_\sigma + j_\tau + L$ even, and $\Pi(j_\sigma, j_\tau, L) = 0$ otherwise. For magnetic multipoles, $\Pi(j_\sigma, j_\tau, L) = 1$ for $\kappa_\sigma \kappa_\tau > 0$, $j_\sigma + j_\tau + L$ even or $\kappa_\sigma \kappa_\tau < 0$, $j_\sigma + j_\tau + L$ odd, and $\Pi(j_\sigma, j_\tau, L) = 0$ otherwise.

$\mathcal{F}_{\sigma\tau}$, $\mathcal{H}_{\sigma\tau}$, $\mathcal{L}_{\sigma\tau}$, and $\mathcal{T}_{\sigma\tau}$ are radial integrals. In the notation used by Rosner and Bhalla [93], they read

$$\mathcal{F}_{f,n} = [L]^{-1/2} \left\{ \sqrt{\frac{L}{L+1}} [(\kappa_f - \kappa) \check{I}_{L+1}^+ + (L+1) \check{I}_{L+1}^-] - \sqrt{\frac{L+1}{L}} [(\kappa_f - \kappa) \check{I}_{L-1}^+ - L \check{I}_{L-1}^-] \right\}, \quad (\text{B6})$$

$$\mathcal{F}_{n,i} = [L]^{-1/2} \left\{ \sqrt{\frac{L}{L+1}} [(\kappa - \kappa_i) \hat{I}_{L+1}^+ + (L+1) \hat{I}_{L+1}^-] - \sqrt{\frac{L+1}{L}} [(\kappa - \kappa_i) \hat{I}_{L-1}^+ - L \hat{I}_{L-1}^-] \right\}, \quad (\text{B7})$$

$$\mathcal{H}_{f,n} = [L]^{-1/2} \{ (\kappa_f - \kappa) [\check{I}_{L+1}^+ + \check{I}_{L-1}^+] + (L+1) \check{I}_{L+1}^- - L \check{I}_{L-1}^- \}, \quad (\text{B8})$$

$$\mathcal{H}_{n,i} = [L]^{-1/2} \{(\kappa - \kappa_i)[\hat{I}_{L+1}^+ + \hat{I}_{L-1}^+] + (L+1)\hat{I}_{L+1}^- - L\hat{I}_{L-1}^-\}, \quad (\text{B9})$$

$$\mathcal{L}_{f,n} = [L]^{1/2} \check{J}_L, \quad \mathcal{L}_{n,i} = [L]^{1/2} \hat{J}_L, \quad (\text{B10})$$

$$\mathcal{T}_{f,n} = \sqrt{\frac{2L+1}{L(L+1)}}(\kappa_f + \kappa)\check{I}_L^+, \quad (\text{B11})$$

$$\mathcal{T}_{n,i} = \sqrt{\frac{2L+1}{L(L+1)}}(\kappa + \kappa_i)\hat{I}_L^+,$$

where

$$\check{I}_L^\pm = \int_0^\infty dr j_L(\omega r) [P_{n_f \kappa_f}(r) T_{n \kappa}(2\lambda r) \pm Q_{n_f \kappa_f}(r) S_{n \kappa}(2\lambda r)], \quad (\text{B12})$$

$$\hat{I}_L^\pm = \int_0^\infty dr j_L(\omega r) [\tilde{\theta}_{n \kappa} Q_{n_i \kappa_i}(r) S_{n \kappa}(2\lambda r) \pm \tilde{\alpha}_{n \kappa} P_{n_i \kappa_i}(r) T_{n \kappa}(2\lambda r)], \quad (\text{B13})$$

$$\check{J}_L = \int_0^\infty dr j_L(\omega r) [P_{n_f \kappa_f}(r) S_{n \kappa}(2\lambda r) + Q_{n_f \kappa_f}(r) T_{n \kappa}(2\lambda r)], \quad (\text{B14})$$

$$\hat{J}_L = \int_0^\infty dr j_L(\omega r) [\tilde{\theta}_{n \kappa} P_{n_i \kappa_i}(r) S_{n \kappa}(2\lambda r) + \tilde{\alpha}_{n \kappa} Q_{n_i \kappa_i}(r) T_{n \kappa}(2\lambda r)]. \quad (\text{B15})$$

$j_L(x)$ is the well-known spherical Bessel function of the first kind.

-
- [1] Z. Zheng, A. M. Weiner, J. H. Marsh, and M. M. Karkhanehchi, *IEEE Photon. Technol. Lett.* **9**, 493 (1997).
- [2] T. W. Hänsch, S. A. Lee, R. Wallenstein, and C. Wieman, *Phys. Rev. Lett.* **34**, 307 (1975); S. A. Lee, R. Wallenstein, and T. W. Hänsch, *ibid.* **35**, 1262 (1975).
- [3] R. J. Fonck, D. H. Tracy, D. C. Wright, and F. S. Tomkins, *Phys. Rev. Lett.* **40**, 1366 (1978).
- [4] L. Safari, P. Amaro, S. Fritzsch, J. P. Santos, and F. Fratini, *Phys. Rev. A* **85**, 043406 (2012).
- [5] S. Zapryagaev, *Phys. Scr. T* **144**, 014053 (2011).
- [6] R. Marrus and R. W. Schmieder, *Phys. Rev. A* **5**, 1160 (1972).
- [7] E. A. Hinds, J. E. Clendenin, and R. Novick, *Phys. Rev. A* **17**, 670 (1978).
- [8] H. Gould and R. Marrus, *Phys. Rev. Lett.* **41**, 1457 (1978); *Phys. Rev. A* **28**, 2001 (1983).
- [9] R. W. Dunford, M. Hass, E. Bakke, H. G. Berry, C. J. Liu, M. L. A. Raphaelian, and L. J. Curtis, *Phys. Rev. Lett.* **62**, 2809 (1989).
- [10] L. Cook, D. Olsgaard, M. Havey, and A. Sieradzan, *Phys. Rev. A* **47**, 340 (1993).
- [11] P. C. Stancil and G. E. Copeland, *J. Phys. B: At. Mol. Opt. Phys.* **27**, 2801 (1994).
- [12] *Laser Spectroscopy*, edited by H. Walter (Springer, Berlin, 1976).
- [13] C. Schwob, L. Jozefowski, B. de Beauvoir, L. Hilico, F. Nez, L. Julien, F. Biraben, O. Acef, J. J. Zondy, and A. Clairon, *Phys. Rev. Lett.* **82**, 4960 (1999).
- [14] B. de Beauvoir, C. Schwob, O. Acef, L. Jozefowski, L. Hilico, F. Nez, L. Julien, A. Clairon, and F. Biraben, *Eur. Phys. J. D* **12**, 61 (2000).
- [15] T. W. Hänsch, *Rev. Mod. Phys.* **78**, 1297 (2006).
- [16] E. G. Drukarev and A. N. Moskalev, *Zh. Eksp. Teor. Fiz.* **73**, 2060 (1977).
- [17] M. Maul, A. Schäfer, W. Greiner, and P. Indelicato, *Phys. Rev. A* **53**, 3915 (1996).
- [18] W. Perrie, A. J. Duncan, H. J. Beyer, and H. Kleinpoppen, *Phys. Rev. Lett.* **54**, 1790 (1985).
- [19] H. Kleinpoppen, A. J. Duncan, H. J. Beyer, and Z. A. Sheikh, *Phys. Scr. T* **72**, 7 (1997).
- [20] S. Seager, D. D. Sasselov, and D. Scott, *Astrophys. J. Lett.* **523**, L1 (1999).
- [21] J. Chluba and R. A. Sunyaev, *Astron. Astrophys.* **446**, 39 (2006).
- [22] T. Tsujibayashi, M. Itoh, J. Azuma, M. Watanabe, O. Arimoto, S. Nakanishi, H. Itoh, and M. Kamada, *Phys. Rev. Lett.* **94**, 076401 (2005).
- [23] P. T. C. So, C. Y. Dong, and B. R. Masters, in *Biomedical Photonics Handbook*, edited by T. Vo-Dinh (CRC, Boca Raton, FL, 2003).
- [24] S. Fujiyoshi, M. Fujiwara, and M. Matsushita, *Phys. Rev. Lett.* **100**, 168101 (2008).
- [25] H. H. Kramers and W. Heisenberg, *Z. Phys.* **31**, 681 (1925).
- [26] I. Waller, *Z. Phys.* **58**, 75 (1928).
- [27] M. Goeppert-Mayer, *Ann. Phys. (Leipzig)* **9**, 273 (1931).
- [28] G. Breit and E. Teller, *Astrophys. J.* **91**, 215 (1940).
- [29] L. Spitzer and J. L. Greenstein, *Astrophys. J.* **114**, 407 (1951).
- [30] J. Shapiro and G. Breit, *Phys. Rev.* **113**, 179 (1959).
- [31] B. A. Zon and L. P. Rapoport, *Pis'ma v ZhETF* **7**, 70 (1968) [Sov. Phys. JETP Lett.] **7**, 52 (1968); B. A. Zon, N. L. Manakov, and L. P. Rapoport, *Zh. Eksp. Teor. Fiz.* **56**, 400 (1969) [Sov. Phys.- JETP] **28**, 480 (1969).
- [32] S. Klarsfeld, *Phys. Lett. A* **30**, 382 (1969).
- [33] J. H. Tung, X. M. Ye, G. J. Salamo, and F. T. Chan, *Phys. Rev. A* **30**, 1175 (1984).
- [34] V. Florescu, *Phys. Rev. A* **30**, 2441 (1984).
- [35] L. Labzowsky, D. Solovyev, G. Plunien, and G. Soff, *Eur. Phys. J. D* **37**, 335 (2006).
- [36] D. Solovyev, V. Sharipov, L. Labzowsky, and G. Plunien, *J. Phys. B: At. Mol. Opt. Phys.* **43**, 074005 (2010).
- [37] F. Bassani, J. J. Forney, and A. Quattropani, *Phys. Rev. Lett.* **39**, 1070 (1977).
- [38] A. Quattropani, F. Bassani, and S. Carillo, *Phys. Rev. A* **25**, 3079 (1982).
- [39] R. J. Drachman, A. K. Bhatia, and A. A. Shabazz, *Phys. Rev. A* **42**, 6333 (1990).
- [40] W. R. Johnson, *Phys. Rev. Lett.* **29**, 1123 (1972).
- [41] S. P. Goldman and G. W. F. Drake, *Phys. Rev. A* **24**, 183 (1981).
- [42] G. W. F. Drake and S. P. Goldman, *Phys. Rev. A* **23**, 2093 (1981).
- [43] F. A. Parpia and W. R. Johnson, *Phys. Rev. A* **26**, 1142 (1982).

- [44] J. P. Santos, F. Parente, and P. Indelicato, *Eur. Phys. J. D* **3**, 43 (1998).
- [45] L. Labzowsky, A. V. Shonin, and D. A. Solov'yev, *J. Phys. B: At. Mol. Opt. Phys.* **38**, 265 (2005); L. N. Labzowsky and A. V. Shonin, *Phys. Lett. A* **333**, 289 (2004).
- [46] U. D. Jentschura and A. Surzhykov, *Phys. Rev. A* **77**, 042507 (2008).
- [47] P. Amaro, J. P. Santos, F. Parente, A. Surzhykov, and P. Indelicato, *Phys. Rev. A* **79**, 062504 (2009).
- [48] X. M. Tong, J. M. Li, L. Kissel, and R. H. Pratt, *Phys. Rev. A* **42**, 1442 (1990).
- [49] A. Surzhykov, P. Koval, and S. Fritzsche, *Phys. Rev. A* **71**, 022509 (2005).
- [50] A. Surzhykov, T. Radtke, P. Indelicato, and S. Fritzsche, *Eur. Phys. J. Spec. Top.* **169**, 29 (2009).
- [51] A. Dalgarno and J. T. Lewis, *Proc. R. Soc. London, Ser. A* **233**, 70 (1955); A. Dalgarno, *Rev. Mod. Phys.* **35**, 522 (1963).
- [52] Y. Gontier and M. Trahin, *Phys. Rev.* **172**, 83 (1968); *Phys. Rev. A* **4**, 1896 (1971); **14**, 1935(E) (1976).
- [53] B. H. Bebb and A. Gold, *Phys. Rev.* **143**, 1 (1966).
- [54] G. W. F. Drake, *Phys. Rev. A* **34**, 2871 (1986).
- [55] P. Amaro, A. Surzhykov, F. Parente, P. Indelicato, and J. P. Santos, *J. Phys. A: Math. Theor.* **44**, 245302 (2011).
- [56] W. R. Johnson, S. A. Blundell, and J. Sapirstein, *Phys. Rev. A* **37**, 307 (1988).
- [57] J. Schwinger, *J. Math. Phys.* **5**, 1606 (1964).
- [58] L. Hostler, *J. Math. Phys. (NY)* **5**, 591 (1964); **5**, 1235 (1964).
- [59] L. Hostler, *J. Math. Phys. (NY)* **11**, 2966 (1970).
- [60] G. S. Adkins and R. F. Hood, *Eur. J. Phys.* **10**, 61 (1989).
- [61] E. Karule, *J. Phys. B: At. Molec. Phys.* **4**, L67 (1971).
- [62] A. Maquet, *Phys. Rev. A* **15**, 1088 (1977).
- [63] J. Avery, T. B. Hansen, M. Wang, and F. Antonsen, *Int. J. Quantum Chem.* **57**, 401 (1996), and references therein.
- [64] E. Holøien, *Phys. Rev.* **104**, 1301 (1956).
- [65] H. Shull and P. O. Löwdin, *J. Chem. Phys.* **30**, 617 (1959).
- [66] M. Rotenberg, *Ann. Phys. (NY)* **62**, 262 (1962); *Adv. At. Mol. Phys.* **6**, 233 (1970).
- [67] E. Foumouo, G. L. Kamta, G. Edah, and B. Piraux, *Phys. Rev. A* **74**, 063409 (2006).
- [68] J. M. Ngoko Djokap, E. Foumouo, M. G. Kwato Njock, X. Urbain, and B. Piraux, *Phys. Rev. A* **81**, 042712 (2010).
- [69] M. S. Mengoué, M. G. Kwato Njock, B. Piraux, Yu. V. Popov, and S. A. Zaytsev, *Phys. Rev. A* **83**, 052708 (2011).
- [70] G. W. F. Drake and S. P. Goldman, *Adv. At. Mol. Phys.* **25**, 393 (1988).
- [71] I. P. Grant and H. M. Quiney, *Adv. At. Mol. Phys.* **23**, 37 (1988); H. M. Quiney, I. P. Grant, and S. Wilson, in *Lecture Notes in Quantum Chemistry*, edited by U. Kaldor (Springer-Verlag, Berlin, 1989), Vol. 52, pp. 307–344; I. P. Grant, in *Relativistic, Quantum Electrodynamics and Weak Interaction Effects in Atoms*, edited by P. J. Mohr, W. R. Johnson, and J. Sucher, AIP Conf. Proc. No. 189 (AIP, New York, 1989), pp. 235–253; in *The Effects of Relativity in Atoms, Molecules, and the Solid State*, edited by S. Wilson, I. P. Grant, and B. L. Gyorffy (Plenum, New York, 1991); I. P. Grant, *Adv. At. Mol. Phys.* **32**, 169 (1994); I. P. Grant, in *Atomic, Molecular and Optical Physics Reference Book*, edited by G. W. F. Drake (AIP, New York, 1996), Chap. 22.
- [72] R. Szmytkowski, *J. Phys. B: At. Mol. Opt. Phys.* **30**, 825 (1997); **30**, 2747(E) (1997).
- [73] R. Szmytkowski, *J. Phys. A: Math. Gen.* **33**, 427 (2000).
- [74] I. P. Grant and H. M. Quiney, *Phys. Rev. A* **62**, 022508 (2000).
- [75] R. Szmytkowski and K. Mielewczyk, *J. Phys. B: At. Mol. Opt. Phys.* **37**, 3961 (2004).
- [76] R. Szmytkowski, *Phys. Rev. A* **65**, 012503 (2001).
- [77] R. Szmytkowski, *J. Phys. B: At. Mol. Opt. Phys.* **35**, 1379 (2002).
- [78] K. Mielewczyk and R. Szmytkowski, *Phys. Rev. A* **73**, 022511 (2006).
- [79] P. Stefańska and R. Szmytkowski, *Int. J. Quantum Chem.* **112**, 1363 (2012).
- [80] R. Szmytkowski and P. Stefańska, *Phys. Rev. A* **85**, 042502 (2012).
- [81] H. M. Tetchou Nganso and M. G. Kwato Njock, *J. Phys. B: At. Mol. Opt. Phys.* **40**, 807 (2007).
- [82] *Handbook of Atomic Molecular and Optical Physics*, edited by G. W. F. Drake (Springer, Berlin, 2006).
- [83] A. I. Akhiezer and V. B. Berestetskii, *Quantum Electrodynamics* (Wiley, New York, 1965).
- [84] D. A. Varshalovich, A. N. Moskalev, and V. K. Khersonskii, *Quantum Theory of Angular Momentum* (World Scientific, Singapore, 1988).
- [85] I. P. Grant, *J. Phys. B: At. Mol. Opt. Phys.* **7**, 1458 (1974).
- [86] *Handbook of Mathematical Functions*, NBS Applied Mathematical Series, edited by M. Abramowitz and I. A. Stegun (National Bureau of Standards, Washington, DC, 1985).
- [87] S. P. Goldman, *Phys. Rev. A* **40**, 1185 (1989).
- [88] C. Szymanowski, V. Véniard, R. Taïeb, and A. Maquet, *Phys. Rev. A* **56**, 700 (1997).
- [89] L. Hostler and R. H. Pratt, *Phys. Rev. Lett.* **10**, 469 (1973).
- [90] R. A. Swainson and G. W. F. Drake, *J. Phys. A: Math. Gen.* **24**, 79 (1991); **24**, 95 (1991); **24**, 1801 (1991).
- [91] M. Pont and R. Shakeshaft, *Phys. Rev. A* **44**, R4110 (1991).
- [92] L. Armstrong, W. R. Fielder, and D. L. Lin, *Phys. Rev. A* **14**, 1114 (1976).
- [93] H. R. Rosner and C. P. Bhalla, *Z. Phys.* **231**, 347 (1970).